Spontaneous emission from a two-level atom in two-band anisotropic photonic crystals

Yaping Yang,[1,2,3] M. Fleischhauer,[2] and Shi-Yao Zhu[3]
[1]*Department of Physics, Tongji University, Shanghai 200092, China*
[2]*Fachbereich Physik, University Kaiserslautern, D-67663 Kaiserslautern, Germany*
[3]*Department of Physics, Hongkong Baptist University, Hong Kong*
(Received 21 May 2003; published 8 October 2003)

We investigate the spontaneous radiation from a two-level atom embedded in a three-dimensional anisotropic photonic crystal with two bands. The properties of the spontaneous emission are dependent strongly on the position of the upper level. The faster and slower decay components can occur in the emitted field, but it does not mean the existence of both accelerated and inhibited components for the atomic population decay. The radiation spectrum is dependent on the location of the observer. We also study the influence of the existence of the two bands on spontaneous emission, Lamb shift, the emitted field, and the radiation spectrum.

DOI: 10.1103/PhysRevA.68.043805 PACS number(s): 42.50.Dv, 32.80.Bx

I. INTRODUCTION

Photonic crystals investigated initially by Yablonovitch and independently by John are periodic dielectric structures, which can lead to one or more than one band gap in the frequencies of electromagnetic radiation allowed to exist and propagate inside the material [1,2]. The electromagnetic field with frequencies being within the band gap cannot propagate in all directions. The dispersion characteristics of radiation waves traveling in a photonic crystal are changed, and the mode density of the electromagnetic field is deformed in comparison with that for free space vacuum field. This is because spontaneous emission from an excited atom is dependent not only on the properties of the atom but also on the nature of the surrounding environment, specifically on the density of electromagnetic vacuum modes. The change of mode density and the inhibition of electromagnetic wave propagation in photonic crystals provide a way to control spontaneous emission, which may facilitate the advancement of optics and optoelectronics, and has many important applications [3]. Thus, the spontaneous emission from an excited atom embedded in photonic crystals has attracted a lot of attention in recent years [4–12]. In the previous studies for atoms embedded in photonic crystals, many interesting effects have been discovered when the resonant transition frequencies of the atoms are near the band edge, for example, localization of light [2,4], photon-atom bound states [5–9], suppression and even complete cancellation of spontaneous emission [8], the enhancement of spontaneous emission interference [7,9], coherent control of spontaneous emission [10], the occurrence of dark lines in spontaneous emission [11], the quantum Zeno effect, the quantum anti-Zeno effect in photonic crystals [12], etc.

In many earlier studies, only one band (usually an upper band) for photonic crystals was considered. When the atomic resonant transition frequency is very close to the edge of one band and the band gap is relatively large, the one-band model is a good approximation. If the band gap is narrow, we must consider both upper and lower bands. In the present paper, we study the spontaneous emission from a two-level atom embedded in an anisotropic photonic crystal with an upper band, a lower band, and a band gap. The influence of the existence of the second band (the lower band) on spontaneous emission, Lamb shift, the emitted field and the radiation spectrum are investigated. As to the time evolution of the atomic population in the excited state, the effect of the lower band is the same as the upper band because of the symmetrical distribution of density of states. Comparing to the single-band case, the coexistence of the upper and lower bands leads to a faster decay of the population due to the stronger coupling between the atomic transition and the electromagnetic modes. The contribution of the upper band to Lamb shift is opposite to that for the lower band, and the Lamb shift in the two-band case is smaller than that in the single-band case. The amplitude of characteristic localized field is reduced due to existence of two bands. In a more special case, the amplitude of the characteristic localized field may be zero, and the singularity due to the localized field may vanish in the radiation spectrum.

Recently, there has been considerable experimental work on radiative emission from active material embedded photonic crystals with pseudogaps [13]. Therefore, the traveling behavior of the emitted field and the radiation spectrum are discussed. Most interestingly, the faster and slower decay components corresponding to the diffusion field and the propagating field, respectively, have then trail in the decay process for the emitted field. Differing from the atomic decay in free space or in a homogeneous medium, the coexistence of the faster and slower decay components of the emitted field in photonic crystals does not mean the existence of both accelerated and reduced decay rates for the atomic decay process of the excited-state population. In addition, the part of the energy of the emitted field with frequencies being within the band gap cannot propagate in photonic crystals, the radiation spectrum of the excited atom in a photonic crystal is more complex, and depends on the location of the observer.

The outline of this paper is as follows. In Sec. II, the model and the basic theory to investigate the spontaneous emission are given. In Sec. III, the properties of the time evolution of the population trapped in the excited state, and the influences of the two bands on the population decay and the Lamb shift are studied in detail. In Sec. IV we discuss the properties of the emitted field and its traveling behavior. The spontaneous spectrum is calculated in Sec. V.

II. BASIC THEORY

We consider a two-level atom with an upper level $|1\rangle$ and a lower level $|0\rangle$ embedded in a three-dimensional anisotropic photonic crystal, which has an upper band, a lower band, and a forbidden gap. The cutoff frequencies of the upper band edge and the lower band edge are ω_{c_1} and ω_{c_2}, respectively. The gap width $\omega_{c_1}-\omega_{c_2}$ is assumed much smaller than ω_{c_1}, ω_{c_2}. The upper level is coupled by vacuum modes to the ground level. The resonant frequency between levels $|1\rangle$ and $|0\rangle$ is ω_1, which is assumed to be near the two band edges. The energy of the lower level $|0\rangle$ is set to be zero. Performing the rotating wave approximation for the interaction, the Hamiltonian of this system takes the form

$$H=\hbar\omega_1|1\rangle\langle 1|+\sum_k \hbar\omega_k b_k^\dagger b_k + i\hbar\sum_k g_k(b_k^\dagger|0\rangle\langle 1|-b_k|1\rangle\langle 0|), \tag{1}$$

where b_k ($b_k^\dagger$) is the annihilation (creation) operator for the kth reservoir mode with frequency ω_k. The coupling constant between the atomic transition $|1\rangle\rightarrow|0\rangle$ and the kth electromagnetic mode is $g_k=\omega_1 d_1/\hbar\sqrt{\hbar/(2\varepsilon_0\omega_k V_0)}\mathbf{e}_k\cdot\mathbf{u}_d$, where k represents both the momentum and polarization of the modes, d_1 and $\mathbf{u}_d$ are the magnitude and unit vector of the atomic dipole moment of the transition, V_0 is the quantization volume, $\mathbf{e}_k$ are the transverse unit vectors for the reservoir modes, and ε_0 is the Coulomb constant. For a three-dimensional anisotropic photonic crystal with an allowed point-group symmetry, the dispersion relation near the two band edges could be expressed approximately [5] by

$$\omega_k=\begin{cases}\omega_{c_1}+C_1|\mathbf{k}-\mathbf{k}_{10}^j|^2 & (\omega_k>\omega_{c_1}),\\ \omega_{c_2}-C_2|\mathbf{k}-\mathbf{k}_{20}^j|^2 & (\omega_k<\omega_{c_2}).\end{cases} \tag{2}$$

Here $\mathbf{k}_{10}^i$ and $\mathbf{k}_{20}^j$ are two finite collections of symmetry related points, which are associated with the upper and lower band edges, respectively. C_1 and C_2 are the model-dependent constants.

We assume the atom initially in the upper level $|1\rangle$, and the radiation field is in the vacuum state. The wave function of the system at arbitrary time t may be written as

$$|\psi(t)\rangle=A_1(t)e^{-i\omega_1 t}|1,\{0\}\rangle+\sum_k B_k(t)e^{-i\omega_k t}|0,\{1_k\}\rangle, \tag{3}$$

with $A_1(0)=1$ and $B_k(0)=0$. The state vector $|1,\{0\}\rangle$ describes the atom in its excited state $|1\rangle$ with no photons in all reservoir modes, and the state vector $|0,\{1_k\}\rangle$ represents the atom in its ground state $|0\rangle$ and a single photon in kth mode with frequency ω_k. From the Schrödinger equation $i\hbar(\partial/\partial t)|\psi(t)\rangle=H|\psi(t)\rangle$, we can obtain the following first-order differential equation for the amplitudes $A_1(t)$ and $B_k(t)$:

$$\frac{\partial}{\partial t}A_1(t)=-\sum_k g_k e^{i(\omega_1-\omega_k)t}B_k(t), \tag{4a}$$

$$\frac{\partial}{\partial t}B_k(t)=g_k e^{-i(\omega_1-\omega_k)t}A_1(t). \tag{4b}$$

Formally integrating Eq. (4b), and then substituting into Eq. (4a), we have

$$\frac{\partial}{\partial t}A_1(t)=-\sum_k g_k^2\int_0^t e^{i(\omega_1-\omega_k)(t-t')}A_1(t')dt'. \tag{5}$$

With the help of the Laplace transform, we can solve the above equation. The Laplace transform $A_1(s)$ for the amplitude $A_1(t)$ is

$$A_1(s)=\frac{1}{s+\Gamma}, \tag{6}$$

where $\Gamma=\Sigma_k g_k^2/[s+i(\omega_k-\omega_1)]$. Using the dispersion relation (2), and converting the mode sum over transverse plane waves into an integral and performing the integral, we have $\Gamma=-i\beta_1^{3/2}/[\sqrt{\omega_{c_1}}+\sqrt{-is-(\omega_1-\omega_{c_1})}]+i\beta_2^{3/2}/[\sqrt{\omega_{c_2}}+\sqrt{is+(\omega_1-\omega_{c_2})}]$, with $\beta_1^{3/2}=(\omega_1 d_1)^2\Sigma_j\sin^2\theta_j/(8\pi\epsilon_0\hbar C_1^{3/2})$ and $\beta_2^{3/2}=(\omega_1 d_1)^2\Sigma_j\sin^2\varphi_j/(8\pi\epsilon_0\hbar C_2^{3/2})$ (see Appendix A). Here θ_j (φ_j) is the angle between the dipole vector of the atom and the jth $\mathbf{k}_{10}^j$ (jth $\mathbf{k}_{20}^j$). The phase angle of s is defined by $-\pi<\arg(s)<\pi$, and the phase angles of $\sqrt{-is-(\omega_1-\omega_{c_1})}$ and $\sqrt{is+(\omega_1-\omega_{c_2})}$ are defined by $-\pi/2<\arg[\sqrt{-is-(\omega_1-\omega_{c_1})}]<\pi/2$, and $-\pi/2<\arg[\sqrt{is+(\omega_1-\omega_{c_2})}]<\pi/2$. The amplitude $A_1(t)$ can then be obtained by the inverse Laplace transform

$$A_1(t)=\frac{1}{2\pi i}\int_{\sigma-i\infty}^{\sigma+i\infty}A_1(s)e^{st}ds, \tag{7}$$

where the real number σ is chosen so that $s=\sigma$ lies to the right of all the singularities (poles and branch points) of the function $A_1(s)$. For the sake of simplicity, we assume $\beta_1=\beta_2=\beta$. With the help of complex function integration and the residue theorem, we can obtain the expression of the amplitude $A_1(t)$,

$$A_1(t)=\sum_j\frac{e^{x_j^{(1)}\beta t}}{G'(x_j^{(1)})}+\sum_j\frac{e^{x_j^{(2)}\beta t}}{F'(x_j^{(2)})}+\sum_j\frac{e^{x_j^{(3)}\beta t}}{K'(x_j^{(3)})} + \frac{1}{\pi}\int_0^\infty\left[\frac{i^{1/2}\sqrt{x}e^{i(\omega_1-\omega_{c_1})t}}{[M(x)\sqrt{\Omega_{c_1}}-i]^2-iM^2(x)x} + \frac{i^{-1/2}\sqrt{x}e^{i(\omega_1-\omega_{c_2})t}}{[N(x)\sqrt{\Omega_{c_2}}+i]^2+iN^2(x)x}\right]e^{-x\beta t}dx, \tag{8}$$

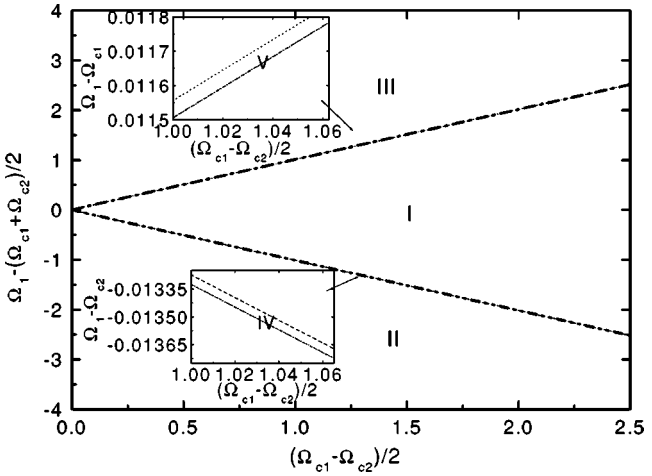

FIG. 1. Five-region distribution for roots with $\omega_{c_1}+\omega_{c_2}=200\beta$.

where these functions $M(x)$, $N(x)$, $G(x)$, $F(x)$, and $K(x)$ are defined in Appendix B. $x_j^{(1)}$are the roots of the equation $G(x)=0$ in region $[\mathrm{Re}(x)>0]$ or $[\Omega_1-\Omega_{c_1}<\mathrm{Im}(x)<\Omega_1-\Omega_{c_2}]$, $x_j^{(2)}$ are the roots of the equation $F(x)=0$ in region $[\mathrm{Re}(x)<0$ and $\mathrm{Im}(x)>(\Omega_1-\Omega_{c_2})]$, and $x_j^{(3)}$ are the roots of $K(x)=0$ in region $[\mathrm{Re}(x)<0$ and $\mathrm{Im}(x)<(\Omega_1-\Omega_{c_1})]$. $G'(x)$, $F'(x)$, and $K'(x)$ are derivatives of those functions $G(x)$, $F(x)$, and $K(x)$, respectively.

From the expression of the amplitude $A_1(t)$, we can see that these roots are important in the study of the dynamical properties of the excited atom. The number and characteristics of these roots are dependent on the separation of the two bands and the relative position of the upper level of the atom from the two band edges. With the help of numerical calculation, we found that there is at most only one root: one pure imaginary root or one complex root. According to the number and the value of the root, we have five regions in the space of $(\Omega_1,\ \Omega_{c_1}-\Omega_{c_2})$. In Fig. 1 we plot the five regions for $\Omega_{c_1}+\Omega_{c_2}=200$. In region I, there is one pure imaginary root with its imaginary part in the range $(\Omega_1-\Omega_{c_1},\Omega_1-\Omega_{c_2})$. In region II, there is one complex root $x^{(2)}$ with a negative real part and an imaginary part larger than $\Omega_1-\Omega_{c_2}$. In region III, we have one complex root $x^{(3)}$ with a negative real part and an imaginary part smaller than $\Omega_1-\Omega_{c_1}$. No root exists in regions IV and V. For the pure imaginary root, it can be proven analytically that there is one and only one purely imaginary root as

$$\Omega_{c_2}+\frac{1}{\sqrt{\Omega_{c_1}}+\sqrt{\Omega_{c_1}-\Omega_{c_2}}}-\frac{1}{\sqrt{\Omega_{c_2}}}$$

$$\leqslant\Omega_1\leqslant\Omega_{c_1}+\frac{1}{\sqrt{\Omega_{c_1}}}-\frac{1}{\sqrt{\Omega_{c_2}}+\sqrt{\Omega_{c_1}-\Omega_{c_2}}}.$$

If $x^{(j)}$ does not exist, the corresponding term in Eq. (8) will be replaced by zero. The last term in the right of Eq. (8) comes from the single-valued branch cut contribution.

The amplitude of the radiation field at a particular space point $\mathbf{r}$ can be calculated from $B_k(t)$ via $A(t)$ in the standard way (see Appendix D) [14]:

$$\mathbf{E}(\mathbf{r},t)=\sum_k\ \sqrt{\frac{\hbar\omega_k}{2\varepsilon_0 V_0}}e^{-i(\omega t-\mathbf{k}\cdot\mathbf{r})}B_k(t)\mathbf{e}_k\,. \tag{9}$$

The emission spectrum $\mathbf{S}(\mathbf{r},\omega)$ can be obtained by using the Fourier transform of the radiation field (see Appendix E),

$$\mathbf{S}(\mathbf{r},\omega)=|\mathbf{F}(\mathbf{r},\omega)|^2, \tag{10}$$

with $\mathbf{F}(\mathbf{r},\omega)=(1/2\pi)\int_0^\infty\mathbf{E}(\mathbf{r},t)e^{i\omega t}dt$.

III. SPONTANEOUS EMISSION

The influence of the two bands on the spontaneous decay can be observed by examining the time evolution of the population in the upper level, which is

$$P(t)=|A_1(t)|^2. \tag{11}$$

The properties of the excited atomic population decay is dependent on the relative position of the upper level from the two bands. When the upper level is in the region I, we have one pure imaginary root $x^{(1)}=ib^{(1)}/\beta$ with $\omega_{c_2}<\omega_1-b^{(1)}<\omega_{c_1}$. The first and last terms in the right of Eq. (8) exist, and other terms are replaced by zero. The corresponding dressed state caused by the interaction between the atom and its own radiation occurs at frequency $\omega_1-b^{(1)}$, which is within the band gap. The dressed state without decay leads to a fractionalized steady-state population trapped in the upper level. The two branch cut contributions yield two quasidressed states at the two band-edge frequencies ω_{c_1} and ω_{c_2}, respectively. The quasidressed states display behavior of power-law decay, and a fractionalized population in the upper level decays to the lower level. When the upper level is in region II (III), we have one complex root $x^{(2)}=(a^{(2)}+ib^{(2)})/\beta$ $[x^{(3)}=(a^{(3)}+ib^{(3)})/\beta]$ with $\omega_1-b^{(2)}<\omega_{c_2}$ $(\omega_1-b^{(3)}>\omega_{c_1})$ and $a^{(2)}<0$ $(a^{(3)}<0)$. The second (third) and last terms in the right of Eq. (8) remain, and other terms vanish. The dressed state occurs at frequency $\omega_1-b^{(2)}$ $(\omega_1-b^{(3)})$. Due to the fact that frequencies of the dressed state and the quasidressed state are within the traveling bands, the upper-level population decays. As the upper level in region II (III), the amplitude of the quasidressed state is negligibly small compared to the dressed state, and the quantum interference between the dressed state and the quasidressed state can be neglected. The spontaneous decay of the excited state displays a simple exponential decay behavior after a very short time. When the upper level is in region IV (V), there is no root. Only the last term in the right of Eq. (8) remains. The quasidressed state at frequency ω_{c_2} (ω_{c_1}) is the only part. The upper-level population decays in the manner of a power-law decay. In Fig. 2, we plot the time evolution of the upper-level population with $\omega_{c_1}=101\beta$ and $\omega_{c_2}=99\beta$ for different relative positions of the upper level from the two bands. Comparing Fig. 2(a) with Fig. 2(b), it is found that the

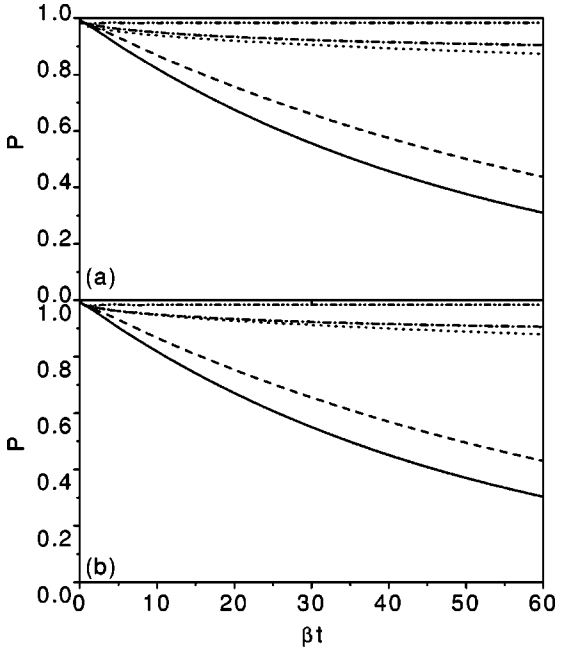

FIG. 2. The excited-state population as a function of the scaled time βt for $\omega_{c_1}=101\beta$, $\omega_{c_2}=99\beta$, and different positions of the upper level. (a) $\omega_1=102\beta$ (solid curve) and 101.5β (dashed curve) in region III, $\omega_1=101.011\,507\beta$ (dotted curve) in region V, $\omega_1=101\beta$ (dash-dotted curve) and 100β (dash-dot-dotted curve) in region I; (b) $\omega_1=98\beta$ (solid curve) and 98.5β (dashed curve) in region II, $\omega_1=98.986\,725\beta$ (dotted curve) in region IV, and $\omega_1=99\beta$ (dash-dotted curve) and 100β (dash-dot-dotted curve) in region I.

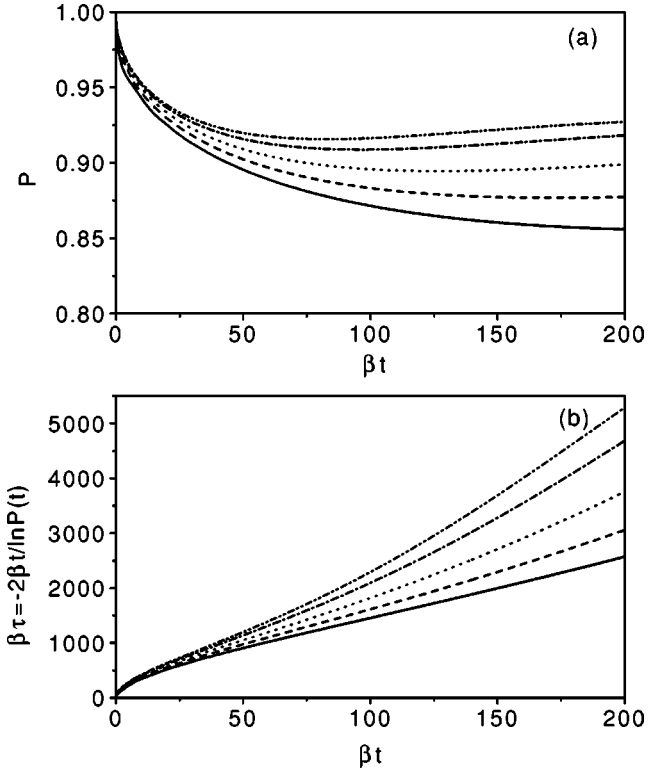

FIG. 3. (a) The excited-state population and (b) the decay time as functions of the scaled time βt for $\omega_1=\omega_{c_1}=101\beta$ and different $\omega_{c_2}=100.5\beta$ (solid curve), 100β (dashed curve), 99β (dotted curve), and 97β (dash-dotted curve), 95β (dash-dot-dotted curve).

time evolution of the excited-state population at symmetrical relative positions of the upper level from the gap center are almost the same. Due to the symmetrical distribution of density of states, the influence of the lower band and the upper band on the atomic dynamic property is the same.

Because of the existence of both the upper and lower bands, the coupling between the atomic transition and the electromagnetic modes strengthens, and the upper-level population decay is faster compared with the single-band case. In Fig. 3 we plot the time evolution and decay time of the excited-state population for fixed positions of the upper band $\omega_{c_1}=101\beta$ and the upper level $\omega_1=101\beta$, and different positions of the lower band. It is obvious that the population decay becomes slower as the width of the band gap increases. When the upper level is near one band edge or within band gap, the influence of the second band on the population decay is more obvious. On the other hand, when the upper level is deeply in one band, the high density of modes causes a strong coupling between the atom and the electromagnetic modes of this band. Consequently, the influence of the another band is small (as shown in Fig. 4).

The steady-state population P_0 can be obtained from Eq. (8). When time goes to infinity, only the first term in Eq. (8) contributes to the population, which stems from the pure imaginary root. When $\omega_1<\omega_{c_2}+[\beta^{3/2}/(\sqrt{\omega_{c_1}}+\sqrt{\omega_{c_1}-\omega_{c_2}})]-(\beta^{3/2}/\sqrt{\omega_{c_2}})$ or $\omega_1>\omega_{c_1}+(\beta^{3/2}/\sqrt{\omega_{c_1}})-[\beta^{3/2}/(\sqrt{\omega_{c_2}}+\sqrt{\omega_{c_1}-\omega_{c_2}})]$, there is no pure imaginary root. As $t\to\infty$, no population is trapped in the upper level, $P_0=0$. As $\omega_{c_2}+[\beta^{3/2}/(\sqrt{\omega_{c_1}}+\sqrt{\omega_{c_1}-\omega_{c_2}})]-(\beta^{3/2}/\sqrt{\omega_{c_2}})\leqslant\omega_1\leqslant\omega_{c_1}+(\beta^{3/2}/\sqrt{\omega_{c_1}})-[\beta^{3/2}/(\sqrt{\omega_{c_2}}+\sqrt{\omega_{c_1}-\omega_{c_2}})]$ (region I), there is only one pure imaginary root $x^{(1)}$. We have $P_0=1/|G'(x^{(1)})|^2$. In Fig. 5, we plot the steady-state population in the upper level as a function of the upper-level frequency with different widths of the band gap. It can be found that the steady-state population increases with the width of the band gap. The position of the upper-level frequency for the maximum upper-level population is close to the center of the band gap.

We consider also the effect of the lower band on the Lamb shift of the atom. The Lamb shift is the difference between the frequency of the dressed state (the frequency of the emitted field) and the upper-level frequency minus the contribution due to mass renormalization. The renormalization contribution is $\beta\mathrm{Im}(x')$, with x' being the root of $\tilde{F}(x)=0$ where $\tilde{F}(x)$ is the same as $F(x)$ with Ω_1 replaced by zero. For different region of the upper-level position, the Lamb shift Δ can be written as

$$\Delta=\beta*\begin{cases}\mathrm{Im}(x^{(1)})-\mathrm{Im}(x') & \text{(region I)}\\ \mathrm{Im}(x^{(2)})-\mathrm{Im}(x') & \text{(region II)}\\ \mathrm{Im}(x^{(3)})-\mathrm{Im}(x') & \text{(region III)}\\ \Omega_1-\Omega_{c_2}-\mathrm{Im}(x') & \text{(region IV)}\\ \Omega_1-\Omega_{c_1}-\mathrm{Im}(x') & \text{(region V).}\end{cases}\tag{12}$$

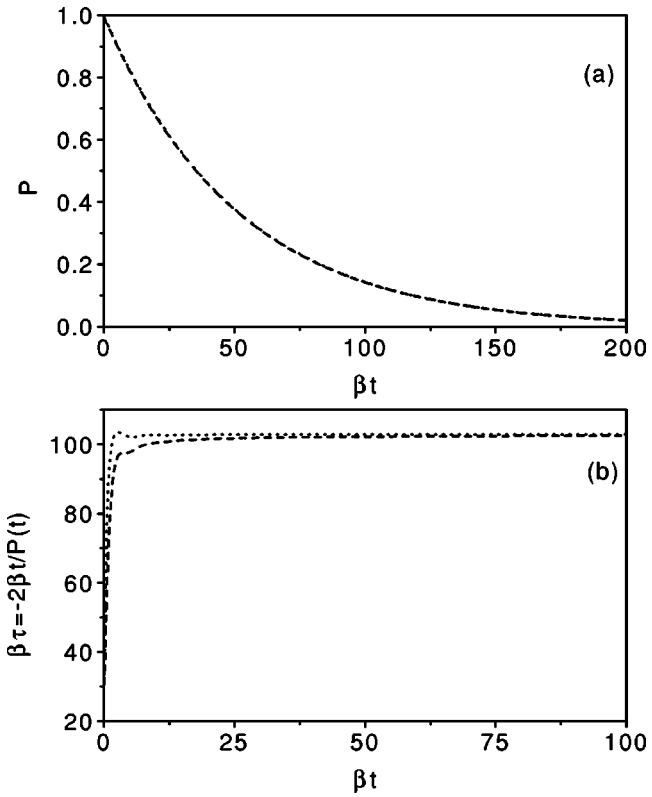

FIG. 4. (a) The excited-state population and (b) the decay time as a function of the scaled time βt for $\omega_1=102\beta$, $\omega_{c_1}=101\beta$, and different $\omega_{c_2}=100.5\beta$ (dashed curve), 95β (dotted curve).

In Fig. 6, we plot the Lamb shift with different width of the band gaps as the upper level is varied from being below the gap to above the gap. In Fig. 6(a), we fix the upper band and change the position of the lower band. When the upper level is within the fixed upper band, the effect of the lower band on the Lamb shift becomes weak as the width of the band gap increases, while the Lamb shift Δ ($\Delta>0$) increases with the width of the band gap. It is to say that the Lamb shift Δ decreases due to existence of the lower band. On the contrary, in Fig. 6(b) we fix the lower band and change the

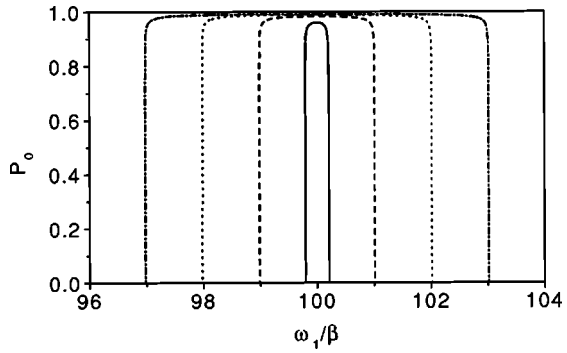

FIG. 5. The steady-state atomic population as a function of the position of the upper level with different band gaps, $\omega_{c_1}=100.2\beta$, $\omega_{c_2}=99.8\beta$ (solid curve), $\omega_{c_1}=101\beta$, $\omega_{c_2}=99\beta$ (dashed curve), $\omega_{c_1}=102\beta$, $\omega_{c_2}=98\beta$ (dotted curve), $\omega_{c_1}=103\beta$, $\omega_{c_2}=97\beta$ (dash-dotted curve).

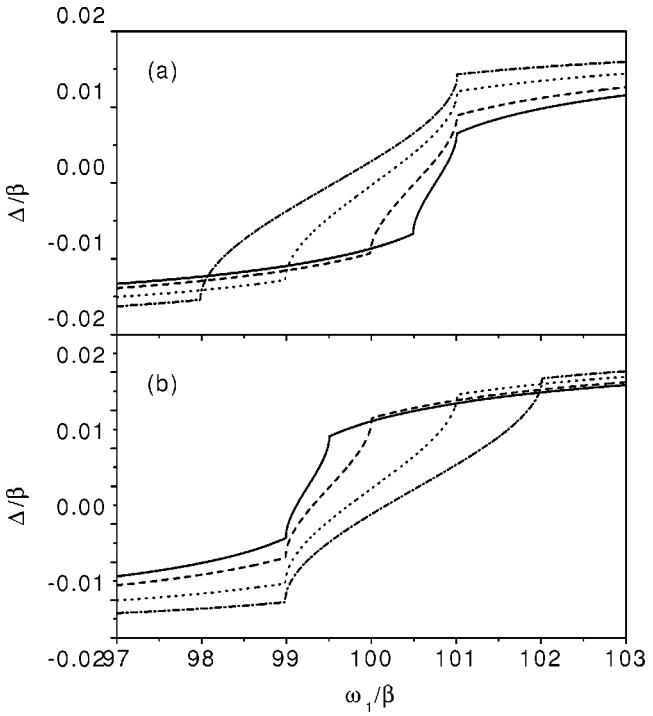

FIG. 6. The Lamb shift in units of β as a function of the upper-level position with different band gaps. (a) $\omega_{c_1}=101\beta$ and $\omega_{c_2}=100.5\beta$ (solid curve), 100β and (dashed curve), 99β (dotted curve), 98β (dash-dotted curve); (b) $\omega_{c_2}=99\beta$ and $\omega_{c_1}=99.5\beta$ (solid curve), 100β (dashed curve), 101β (dotted curve), and 102β (dash-dotted curve).

position of the upper band, and the Lamb shift Δ ($\Delta<0$) decreases with the width of the band gap as the upper level within the lower band. The upper band causes the Lamb shift Δ increasing (the absolute value $|\Delta|$ of the Lamb shift decreasing). Due to the opposite effects for the upper and lower bands, the absolute value $|\Delta|$ of the Lamb shift Δ in the two-band case is more smaller than that in the single-band case.

IV. THE EMITTED FIELD

From Eqs. (8) and (9) we can calculate the emission field under the approximation $\mathbf{k}\cdot\mathbf{r}\gg 1$ [14]. Corresponding to four terms of Eq. (8), the radiated field can be also written as the sum of four parts,

$$\mathbf{E}(\mathbf{r},t)=\mathbf{E}^{(1)}(\mathbf{r},t)+\mathbf{E}^{(2)}(\mathbf{r},t)+\mathbf{E}^{(3)}(\mathbf{r},t)+\mathbf{E}^{(4)}(\mathbf{r},t). \tag{13}$$

$\mathbf{E}^{(1)}(\mathbf{r},t)$ comes from the pure imaginary root $x^{(1)}$, and $\mathbf{E}^{(2)}(\mathbf{r},t)$ [or $\mathbf{E}^{(3)}(\mathbf{r},t)$] stems from the complex root $x^{(2)}$ ($x^{(3)}$). If the pure imaginary root (or the complex root) does not exist, the relevant term in Eq. (13) will be replaced by zero. $\mathbf{E}^{(4)}(\mathbf{r},t)$ comes from the last term (the power-law-decay term) in Eq. (8) and always exists.

When the upper level is within region I, we have one pure imaginary root $x^{(1)}=ib^{(1)}/\beta$, and $\mathbf{E}(\mathbf{r},t)=\mathbf{E}^{(1)}(\mathbf{r},t)+\mathbf{E}^{(4)}(\mathbf{r},t)$. From Eqs. (D11), (D12), and (D15) we can rewrite the emission field $\mathbf{E}(\mathbf{r},t)$ as follows:

$$\mathbf{E}(\mathbf{r},t)=\mathbf{E}_{l1}^{(1)}(\mathbf{r},t)+\mathbf{E}_{l2}^{(1)}(\mathbf{r},t)+\mathbf{E}_{d1}(\mathbf{r},t)+\mathbf{E}_{d2}^{(1)}(\mathbf{r},t), \tag{14}$$

with

$$\mathbf{E}_{l1}^{(1)}(\mathbf{r},t)=\frac{\mathbf{E}_{10}(\mathbf{r})}{G'(x^{(1)})}\frac{\pi}{C_1}e^{-i(\omega_1-b^{(1)})t-r/l_1}\Theta\left(t-\frac{r}{v_{f1}^{(1)}}\right),$$

$$\mathbf{E}_{l2}^{(1)}(\mathbf{r},t)=-\frac{\mathbf{E}_{20}(\mathbf{r})}{G'(x^{(1)})}\frac{\pi}{C_2}e^{-i(\omega_1-b^{(1)})t-r/l_2}\Theta\left(t-\frac{r}{v_{f2}^{(1)}}\right),$$

$$\mathbf{E}_{d1}(\mathbf{r},t)=\mathbf{E}^{(4)}(\mathbf{r},t),$$

$$\mathbf{E}_{d2}^{(1)}(\mathbf{r},t)=\frac{\mathbf{E}_{10}(\mathbf{r})}{G'(x^{(1)})}e^{\phi_1}J_1(r,t,x^{(1)})+\frac{\mathbf{E}_{20}(\mathbf{r})}{G'(x^{(1)})}e^{\phi_2}J_2(r,t,x^{(1)}),$$

$$\mathbf{E}_{10}(\mathbf{r})=\frac{\omega_1 d_1}{8\pi^2\varepsilon_0 ri}\sum_j e^{i\mathbf{k}_{10}^j\cdot\mathbf{r}}\left[\mathbf{u}_d-\frac{\mathbf{k}_{10}^j(\mathbf{k}_{10}^j\cdot\mathbf{u}_d)}{(k_{10}^j)^2}\right],$$

$$\mathbf{E}_{20}(\mathbf{r})=\frac{\omega_1 d_1}{8\pi^2\varepsilon_0 ri}\sum_j e^{i\mathbf{k}_{20}^j\cdot\mathbf{r}}\left[\mathbf{u}_d-\frac{\mathbf{k}_{20}^j(\mathbf{k}_{20}^j\cdot\mathbf{u}_d)}{(k_{20}^j)^2}\right],$$

$$J_1(r,t,x)=\int_{-\infty}^{\infty}\frac{[\rho e^{(3/4)\pi i}+(r/2C_1t)]e^{-C_1t\rho^2}}{(\omega_{c_1}-\omega_1-ix\beta)+C_1\left(\rho e^{(3/4)\pi i}+\frac{r}{2C_1t}\right)^2}d\rho,$$

$$J_2(r,t,x)=\int_{-\infty}^{\infty}\frac{\left(\rho e^{-(3/4)\pi i}-\frac{r}{2C_2t}\right)e^{-C_2t\rho^2}}{(\omega_1+ix\beta-\omega_{c_2})+C_2\left(\rho e^{-(3/4)\pi i}-\frac{r}{2C_2t}\right)^2}d\rho.$$

Here $\phi_1=-i[\omega_{c_1}t-(r^2/4C_1t)]+\frac{1}{4}\pi i$, $\phi_2=-i[\omega_{c_2}t+(r^2/4C_2t)]-\frac{1}{4}\pi i$, and $\Theta(x)$ is the Heaviside step function. The frequency of both the fields $\mathbf{E}_{l1}^{(1)}(\mathbf{r},t)$ and $\mathbf{E}_{l2}^{(1)}(\mathbf{r},t)$ is $\omega_1-b^{(1)}$, which is within band gap. Obviously, those fields represent localized fields without decay in time. The amplitudes of the localized fields $\mathbf{E}_{l1}^{(1)}(\mathbf{r},t)$ and $\mathbf{E}_{l2}^{(1)}(\mathbf{r},t)$ drop exponentially with increasing distance from the atom as e^{-r/l_1} and e^{-r/l_2}, respectively. The localization lengths are $l_1=\sqrt{C_1/(\omega_{c_1}-\omega_1+b^{(1)})}$ and $l_2=\sqrt{C_2/(\omega_1-\omega_{c_2}-b^{(1)})}$, and the front velocities of the localized fields are $v_{f1}^{(1)}=2\sqrt{C_1(\omega_{c_1}-\omega_1+b^{(1)})}$ and $v_{f2}^{(1)}=2\sqrt{C_2(\omega_1-\omega_{c_2}-b^{(1)})}$. From the calculation of the localized fields, $\mathbf{E}_{l1}^{(1)}(\mathbf{r},t)$ and $\mathbf{E}_{l2}^{(1)}(\mathbf{r},t)$ come from the contribution of the upper and lower bands, respectively, while $\mathbf{E}_{d1}(\mathbf{r},t)$ and $\mathbf{E}_{d2}^{(1)}(\mathbf{r},t)$ are the diffusion fields, which have power-law decay and are without fixed phase difference between two space points. The expression of $\mathbf{E}_{d1}(\mathbf{r},t)$ is given in Eq. (D15), which comes from the two branch-point contributions, while $\mathbf{E}_{d2}^{(1)}(\mathbf{r},t)$ comes from the coherent term $e^{x^{(1)}\beta t}/G'(x^{(1)})$ in Eq. (8).

Supposing the symmetry in $\mathbf{k}$ space around points $\mathbf{k}_{10}^j$ are the same as related to $\mathbf{k}_{20}^j$, we have $\mathbf{E}_{10}(\mathbf{r})=\mathbf{E}_{20}(\mathbf{r})$. The phase difference between the localized fields $\mathbf{E}_{l1}^{(1)}(\mathbf{r},t)$ and $\mathbf{E}_{l2}^{(1)}(\mathbf{r},t)$ is π. Consequently, the amplitude of the localized field $\mathbf{E}_{l1}^{(1)}(\mathbf{r},t)+\mathbf{E}_{l2}^{(1)}(\mathbf{r},t)$ becomes small due to existence of the two bands. For special cases $C_1=C_2=C$ and $\omega_1=\omega_0=(\omega_{c_1}+\omega_{c_2})/2+\beta^{3/2}/[\sqrt{\omega_{c_1}}+\sqrt{(\omega_{c_1}-\omega_{c_2})/2}]-\beta^{3/2}/[\sqrt{\omega_{c_2}}+\sqrt{(\omega_{c_1}-\omega_{c_2})/2}]$, we have $l_1=l_2$, $v_{f1}^{(1)}=v_{f2}^{(1)}$, $\mathbf{E}_{l1}^{(1)}(\mathbf{r},t)+\mathbf{E}_{l2}^{(1)}(\mathbf{r},t)=0$. This result is different from that for single-band case. We would like to emphasize that the population calculation is exact, while in the calculation for the field an approximation $\mathbf{k}\cdot\mathbf{r}\gg 1$ is taken, i.e., the result for the radiation field is far away from the atom. The vanishing of the far away field does not mean no field very near the atom. Therefore, we have that the characteristic localized field far away from the atom may vanish and the steady-state population trapped in the upper level has the maximum.

When the upper level gets into region II, we have only one complex root $x^{(2)}=(a^{(2)}+ib^{(2)})/\beta$ with $\omega_1-b^{(2)}<\omega_{c_2}$ and $a^{(2)}<0$. The radiation field $\mathbf{E}(\mathbf{r},t)=\mathbf{E}^{(2)}(\mathbf{r},t)+\mathbf{E}^{(4)}(\mathbf{r},t)$ and can be rewritten as [see Eq. (D13)]

$$\mathbf{E}(\mathbf{r},t)=\mathbf{E}_{ld}^{(2)}(\mathbf{r},t)+\mathbf{E}_{p}^{(2)}(\mathbf{r},t)+\mathbf{E}_{d1}(\mathbf{r},t)+\mathbf{E}_{d2}^{(2)}(\mathbf{r},t), \tag{15}$$

with

$$\mathbf{E}_{ld}^{(2)}(\mathbf{r},t)=\frac{\mathbf{E}_{10}(\mathbf{r})}{F'(x^{(2)})}\frac{\pi}{C_1}\times e^{-i(\omega_1+ix^{(2)}\beta)t-r\sqrt{(\omega_{c_1}-\omega_1-ix^{(2)}\beta)/C_1}}\times\Theta\left(t-\frac{r}{v_{f1}^{(2)}}\right),$$

$$\mathbf{E}_{p}^{(2)}(\mathbf{r},t)=\frac{\mathbf{E}_{20}(\mathbf{r})}{F'(x^{(2)})}\frac{\pi}{C_2}\times e^{-i(\omega_1-b^{(2)})(t-r/v_p^{(2)})+a^{(2)}(t-r/v_e^{(2)})}\Theta\left(t-\frac{r}{v_{f2}^{(2)}}\right),$$

$$\mathbf{E}_{d1}(\mathbf{r},t)=\mathbf{E}^{(4)}(\mathbf{r},t),$$

$$\mathbf{E}_{d2}^{(2)}(\mathbf{r},t)=\frac{\mathbf{E}_{10}(\mathbf{r})}{F'(x^{(2)})}e^{\phi_1}J_1(r,t,x^{(2)})+\frac{\mathbf{E}_{20}(\mathbf{r})}{F'(x^{(2)})}e^{\phi_2}J_2(r,t,x^{(2)}),$$

where $v_p^{(2)}=(\omega_1-b^{(2)})\sqrt{C_2}/\mathrm{Im}(\sqrt{\omega_1-\omega_{c_2}+ix^{(2)}\beta})$, the energy velocity $v_e^{(2)}=-a^{(2)}\sqrt{C_2}/\mathrm{Re}(\sqrt{\omega_1-\omega_{c_2}+ix^{(2)}\beta})$, and the front velocities $v_{f1}^{(2)}=2\sqrt{C_1}(\mathrm{Re}$

$-\mathrm{Im})\sqrt{\omega_{c_1}-\omega_1-ix^{(2)}\beta}$ and $v_{f2}^{(2)}=-2\sqrt{C_2}(\mathrm{Re}+\mathrm{Im})\sqrt{\omega_1-\omega_{c_2}+ix^{(2)}\beta}$. The frequency of both $\mathbf{E}_{ld}^{(2)}(\mathbf{r},t)$ and $\mathbf{E}_p^{(2)}(\mathbf{r},t)$ is $\omega_1-b^{(2)}$, which is within the lower band. $\mathbf{E}_{ld}^{(2)}(\mathbf{r},t)$ comes from the contribution of the upper band, and is localized around the atom. If the lower band does not exist, the frequency will be in band gap, and the field $\mathbf{E}_{ld}^{(2)}(\mathbf{r},t)$ will be localized field without time decay. Now the lower band exists, and the frequency of $\mathbf{E}_{ld}^{(2)}(\mathbf{r},t)$ is within the lower band. In result, the amplitude of $\mathbf{E}_{ld}^{(2)}(\mathbf{r},t)$ drops exponentially with increasing time and distance from the atom, i. e., $\mathbf{E}_{ld}^{(2)}(\mathbf{r},t)$ is a localized decaying field. For large time t or distance r, the amplitude of $\mathbf{E}_{ld}^{(2)}(\mathbf{r},t)$ will be very small, and can be neglected. $\mathbf{E}_p^{(2)}(\mathbf{r},t)$ stems from the contribution of the lower band. It represents a propagating field, which can travel away coherently from the atom in the form of a traveling pulse with the energy velocity $v_e^{(2)}$. $\mathbf{E}_{d1}(\mathbf{r},t)$ and $\mathbf{E}_{d2}^{(2)}(\mathbf{r},t)$ represent the diffusion fields.

Similarly, when the upper level gets into region III, we can obtain one complex root $x^{(3)}=(a^{(3)}+ib^{(3)})/\beta$ with $\omega_1-b^{(3)}>\omega_{c_1}$ and $a^{(3)}<0$. The radiation field $\mathbf{E}(\mathbf{r},t)=\mathbf{E}^{(3)}(\mathbf{r},t)+\mathbf{E}^{(4)}(\mathbf{r},t)$ and can be rewritten as [see Eq. (D14)]

$$\mathbf{E}(\mathbf{r},t)=\mathbf{E}_p^{(3)}(\mathbf{r},t)+\mathbf{E}_{ld}^{(3)}(\mathbf{r},t)+\mathbf{E}_{d1}(\mathbf{r},t)+\mathbf{E}_{d2}^{(3)}(\mathbf{r},t), \tag{16}$$

with

$$\mathbf{E}_p^{(3)}(\mathbf{r},t)=\frac{\mathbf{E}_{20}(\mathbf{r})}{K'(x^{(3)})}\frac{\pi}{C_1}e^{-i(\omega_1-b^{(3)})(t-r/v_p^{(3)})+a^{(2)}(t-r/v_e^{(3)})}\times\Theta\left(t-\frac{r}{v_{f1}^{(3)}}\right),$$

$$\mathbf{E}_{ld}^{(3)}(\mathbf{r},t)=-\frac{\mathbf{E}_{20}(\mathbf{r})}{K'(x^{(3)})}\frac{\pi}{C_2}\times e^{-i(\omega_1+ix^{(3)}\beta)t-r\sqrt{(\omega_1-\omega_{c_2}+ix^{(3)}\beta)/C_2}}\times\Theta\left(t-\frac{r}{v_{f2}^{(3)}}\right),$$

$$\mathbf{E}_{d1}(\mathbf{r},t)=\mathbf{E}^{(4)}(\mathbf{r},t),$$

$$\mathbf{E}_{d2}^{(3)}(\mathbf{r},t)=\frac{\mathbf{E}_{10}(\mathbf{r})}{K'(x^{(3)})}e^{\phi_1}J_1(r,t,x^{(3)})+\frac{\mathbf{E}_{20}(\mathbf{r})}{K'(x^{(3)})}e^{\phi_2}J_2(r,t,x^{(3)}).$$

Here $v_p^{(3)}=(\omega_1-b^{(3)})\sqrt{C_1}/\mathrm{Im}(\sqrt{\omega_{c_1}-\omega_1-ix^{(3)}\beta})$, the energy velocity $v_e^{(3)}=-a^{(3)}\sqrt{C_1}/\mathrm{Re}(\sqrt{\omega_{c_1}-\omega_1-ix^{(3)}\beta})$, and the front velocities $v_{f1}^{(3)}=2\sqrt{C_1}/(\mathrm{Im}-\mathrm{Re})\sqrt{\omega_{c_1}-\omega_1-ix^{(3)}\beta}$ and $v_{f2}^{(3)}=2\sqrt{C_2}/(\mathrm{Im}+\mathrm{Re})\sqrt{\omega_1-\omega_{c_2}+ix^{(3)}\beta}$. The frequency of both fields $\mathbf{E}_p^{(3)}(\mathbf{r},t)$ and $\mathbf{E}_{ld}^{(3)}(\mathbf{r},t)$ is $\omega_1-b^{(3)}>\omega_{c_1}$, which is within the upper band. $\mathbf{E}_p^{(3)}(\mathbf{r},t)$ comes from the contribution of the upper band, and represents a propagating field with the energy velocity $v_e^{(3)}$. $\mathbf{E}_{ld}^{(3)}(\mathbf{r},t)$ is the localized decayed field and can be neglected. $\mathbf{E}_{d1}(\mathbf{r},t)$ and $\mathbf{E}_{d2}^{(3)}(\mathbf{r},t)$ are the diffusion fields.

As the upper level is in region IV or V, no pure imaginary or complex root exists. The emitted field $\mathbf{E}(\mathbf{r},t)=\mathbf{E}^{(4)}(\mathbf{r},t)=\mathbf{E}_{d1}(\mathbf{r},t)$. Only diffusion field exists in regions IV or V. Regions IV and V are caused by the anisotropic dispersion relation and do not exist for an isotropic dispersion relation. For isotropic case, the one-dimensional dispersion relation results in a singularity in the density of state (DOS), and any weak potential will lead to localization [15]. So localized field always exists in the isotropic case. For anisotropic case, there is no singularity in the DOS, and localization requires a potential larger than a certain value [15]. When the upper level moves from gap into the upper (or lower) band, the frequency of the localized field approaches ω_{c_1} (or ω_{c_2}). When the frequency of the localized field is ω_{c_1} (or ω_{c_2}), the localized field disappears, and diffusion field appears, but not a coherent propagating field because the number of electromagnetic modes near the atomic transition frequency is still not large enough.

Although both of the fields $\mathbf{E}_{d1}(\mathbf{r},t)$ and $\mathbf{E}_{d2}(\mathbf{r},t)$ are the diffusion fields, their contributions to the emitted field in different region of the upper level are different. In Fig. 7 we plot the amplitudes of the diffusion fields $\mathbf{E}_{d1}(\mathbf{r},t)$ and $\mathbf{E}_{d2}(\mathbf{r},t)$ as functions of the position of the upper level for the fixed distance from atom $r=r_0=\sqrt{C/\beta}$ and at the fixed time $t=t_0=5/\beta$. In Fig. 7(a) it is shown that the amplitudes of $\mathbf{E}_{d1}(\mathbf{r},t)$ in regions IV and V are almost constant and extremely strong (several hundred times stronger than in other regions) due to the existence of only $\mathbf{E}_{d1}(\mathbf{r},t)$. The amplitude of the diffusion field $\mathbf{E}_{d2}(\mathbf{r},t)$ is zero for the upper level being in regions IV and V, but, it is not zero and much larger than the amplitude of $\mathbf{E}_{d1}(\mathbf{r},t)$ for the upper level being in regions I–III [see Fig. 7(b)]. When the upper level is far away from the regions IV and V, the amplitude of $\mathbf{E}_{d2}(\mathbf{r},t)$ is small [but much larger than $\mathbf{E}_{d1}(\mathbf{r},t)$] because the diffusion field $\mathbf{E}_{d2}(\mathbf{r},t)$ has already decayed at time t_0.

From the above discussion we know that the main parts of the emission field can be written as

$$\mathbf{E}(\mathbf{r},t)\simeq\begin{cases}\mathbf{E}_{l1}^{(1)}(\mathbf{r},t)+\mathbf{E}_{l2}^{(1)}(\mathbf{r},t)+\mathbf{E}_{d2}^{(1)}(\mathbf{r},t) & \text{(region I)}\\ \mathbf{E}_p^{(2)}(\mathbf{r},t)+\mathbf{E}_{d2}^{(2)}(\mathbf{r},t) & \text{(region II)}\\ \mathbf{E}_p^{(3)}(\mathbf{r},t)+\mathbf{E}_{d2}^{(3)}(\mathbf{r},t) & \text{(region III)}\\ \mathbf{E}_{d1}(\mathbf{r},t) & \text{(regions IV, V).}\end{cases} \tag{17}$$

When the upper level goes deeply into the lower or upper bands (region II or III), the population trapped in the excited state has an exponential decay after a very short time. In a free space, the exponential decay $e^{t/\tau}$ of the atomic excited state means that the emission field is a propagating field in form of $A/re^{-i\omega(t-r/v_p)-(t-r/v_e)/\tau}\Theta(t-r/v_f)$ with a fixed

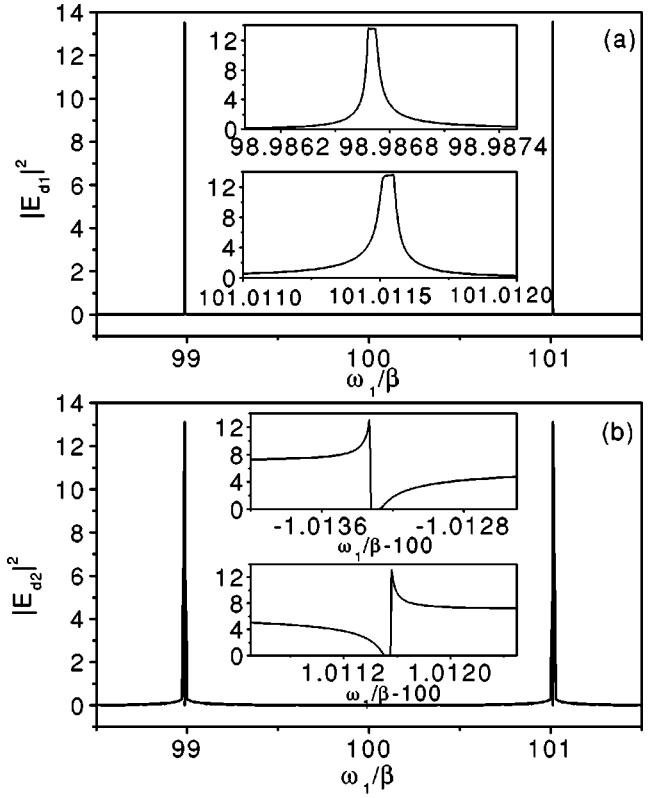

FIG. 7. The amplitude square (in arbitrary unit) of the diffusion field (a) E_{d1} and (b) E_{d2} as function of the transition frequency ω_1 with $\omega_{c_1}=101\beta$, $\omega_{c_2}=99\beta$, $r\sqrt{\beta/C}=1$, and $\beta t=5$.

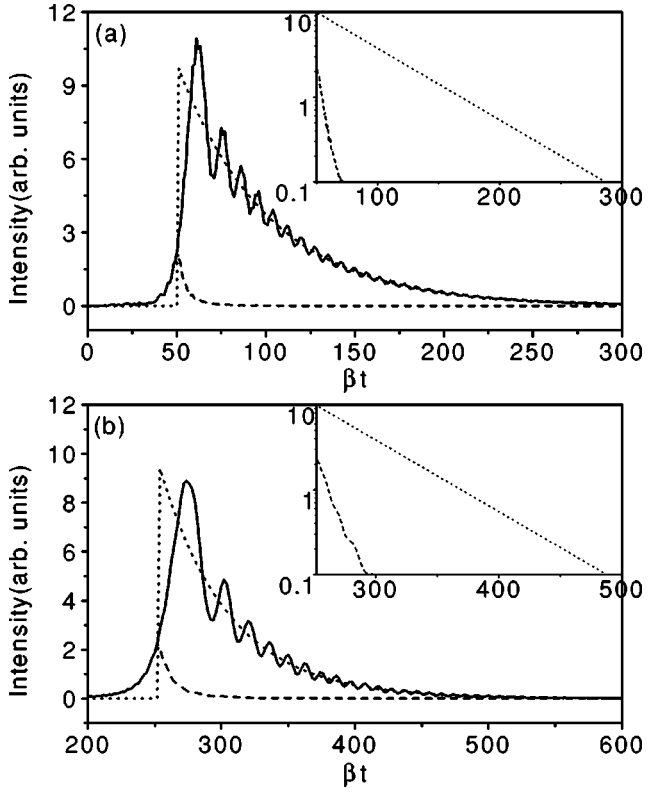

FIG. 8. The time evolution of the intensity (in arbitray unit) of the total emitted field (solid line), the propagating field (dotted line), and the diffusion field (dashed line) for $\omega_{c_1}=101\beta$, $\omega_{c_2}=99\beta$, and $\omega_1=102\beta$ with different distances from atom r. (a) $r(\beta/A)^{1/2}=100$ and (b) $r(\beta/A)^{1/2}=500$.

frequency ω, a fixed phase velocity v_p, a fixed energy velocity v_e, and a fixed front velocity v_f. In the free space the maximum amplitude A does not decay with the distance from the atom due to $v_e=v_f$, and all energy of the emitted field can coherently propagate out in the form of a traveling pulse. The so-called ''coherently'' means that the phase difference between any two points in the space is fixed. For an atom in a photonic crystal, the relation between the population of the upper level and the emitted field is more complex. From Eq. (17) we can see that there are two different fields in the emitted field, the propagating field $\mathbf{E}_p(\mathbf{r},t)$ and the diffusion field $\mathbf{E}_{d2}(\mathbf{r},t)$. Both of $\mathbf{E}_p^{(2)}(\mathbf{r},t)$ and $\mathbf{E}_{d2}^{(2)}(\mathbf{r},t)$ [or $\mathbf{E}_p^{(3)}(\mathbf{r},t)$ and $\mathbf{E}_{d2}^{(3)}(\mathbf{r},t)$] come from the same coherent decay term $e^{x^{(2)}\beta t}/F'(x^{(2)})$ [or $e^{x^{(3)}\beta t}/K'(x^{(3)})$] in Eq. (8). The time evolutions of the emitted field for different space points are plotted in Fig. 8. At a space point, one could see first the diffusion field, and then the propagating field. In the decay process, the quantum interference between the propagating field and the diffusion field leads to the oscillation of the field intensity. The characteristic decay time of the propagating field is a constant and the same as that of the population of the excited state. The diffusion field displays power-law decay. In the first decay stage the intensity of the diffusion field drops fast, and the relevant decay time is shorter than that of the propagating field (see the inset scheme in Fig. 8). Thus the emitted field is composed of a fast decay part (the diffusion field) and a slow decay part (the propagating field). In addition, it can be proven analytically that the energy velocity is larger than the front velocity for the propagating field, $v_e^{(2)}>v_{f2}^{(2)}$ and $v_e^{(3)}>v_{f1}^{(3)}$ (see Appendix F). The maximum amplitude of the propagating field decays with the distance from the atom. It is to say that not all energy of the propagating field can coherently propagate out. During the process of traveling, the energy of the propagating field is partly transferred into the diffusion field due to the influence of photonic crystals. However, the emitted field is mainly a propagating field as the upper level is deep within either of the two transmission bands, and the amplitude of the propagating field is larger than that of the diffusion field. At the same time, the decay of the diffusion field slows down as the distance from the atom increases [comparing Fig. 8(a) with Fig. 8(b)].

V. SPONTANEOUS EMISSION SPECTRUM

Photonic crystals can affect strongly the spontaneous spectrum of the excited atom. From Appendix E the radiation spectrum $S(\mathbf{r},\omega)$ can be written as

$$\mathbf{S(r,\omega)}=\begin{cases}|\mathbf{F}_1(\mathbf{r},\omega)+\mathbf{F}_4(\mathbf{r},\omega)|^2 & \text{(region I)}\\ |\mathbf{F}_2(\mathbf{r},\omega)+\mathbf{F}_4(\mathbf{r},\boldsymbol{\omega})|^2 & \text{(region II)}\\ |\mathbf{F}_3(\mathbf{r},\omega)+\mathbf{F}_4(\mathbf{r},\omega)|^2 & \text{(region III)}\\ |\mathbf{F}_4(\mathbf{r},\omega)|^2 & \text{(regions IV, V)}.\end{cases} \tag{18}$$

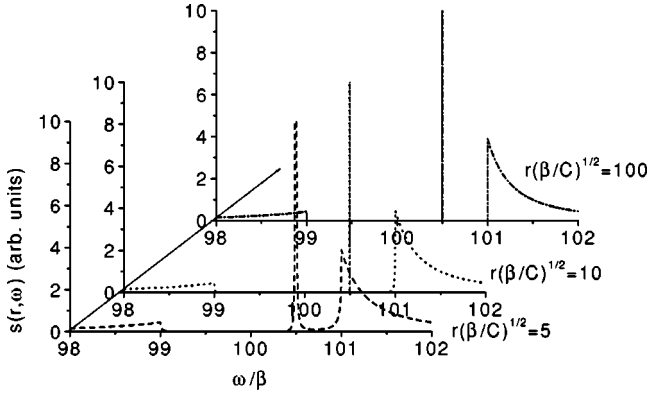

FIG. 9. The spectra of spontaneous emission from the excited atom for $\omega_{c_1}=101\beta$, $\omega_{c_2}=99\beta$, and $\omega_1=100.5\beta$ (region I) with different distances from atom.

Where the functions $\mathbf{F}_1(\mathbf{r},\omega)$, $\mathbf{F}_2(\mathbf{r},\omega)$, $\mathbf{F}_3(\mathbf{r},\omega)$ and $\mathbf{F}_4(\mathbf{r},\omega)$ are given in Appendix E [see Eqs. (E3)–(E6)]. If the upper level is within region I, II, or III, $\mathbf{F}_4(\mathbf{r},\omega)$ will be negligibly small compared to $\mathbf{F}_{1,2,3}(\mathbf{r},\omega)$. In the following discussion, we assume $C_1=C_2=C$ and $\mathbf{E}_{10}(\mathbf{r})=\mathbf{E}_{20}(\mathbf{r})=\mathbf{E}_0(\mathbf{r})$.

When the upper level is within region I, there are the localized field and the diffusion field in the emitted field. The emission spectrum is composed of one singularity due to the characteristic localized mode and two small peaks at the two band edges corresponding to the diffusion field. In Fig. 9, we plot the emission spectra $s(r,\omega)=\mathrm{S}(\mathbf{r},\omega)|C|^2/|\mathbf{E}_0(\mathbf{r})|^2$ for $\omega_{c_1}=101\beta$, $\omega_{c_2}=99\beta$, $\omega_1=100.5\beta$, and different distance from the atom r. In free space, the emission spectrum of two-level excited atom is independent on the position of the observer in space. For the present case, the radiation spectrum is more complex due to the influence of photonic crystal. The part of the emitted field with the frequency being in the band gap is localized, the corresponding energy is limited near the atom, and the amplitude drops exponentially with increasing distance from the atom. For large r, the part of the emission spectrum with frequencies being in band gap is composed of one line corresponding to the characteristic localized mode. Because all energy of the emitted field with frequency being in the two bands can propagate out, the corresponding part of the emission spectrum does not change with the distance from the atom. In results, the total emission spectrum is dependent on the distance from the atom (the location of the observer). When the upper level is more near the band edge ω_{c_1} (or ω_{c_2}), the peak at frequency ω_{c_1} (or ω_{c_2}) is larger than another peak at frequency ω_{c_2} (or ω_{c_1}).

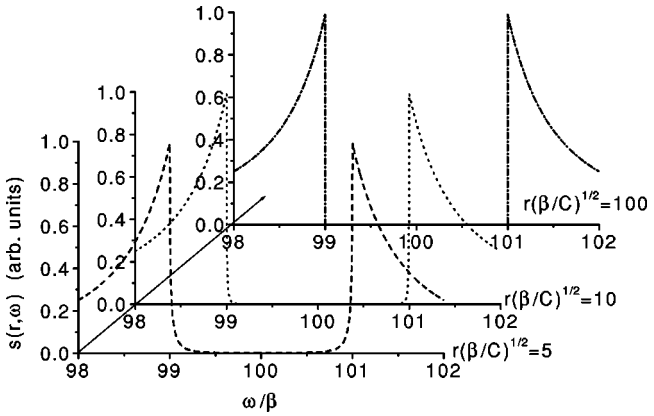

FIG. 10. The spectra of spontaneous emission from the excited atom for $\omega_{c_1}=101\beta$, $\omega_{c_2}=99\beta$, and $\omega_1=99.9991735\beta$ (region I) with different distances from atom.

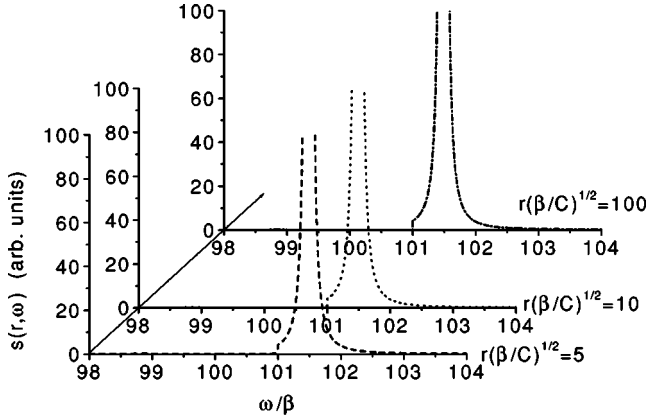

FIG. 11. The spectra of spontaneous emission from the excited atom for $\omega_{c_1}=101\beta$, $\omega_{c_2}=99\beta$, and $\omega_1=101.5\beta$ (region III) with different distances from atom.

For special case $\omega_1=\omega_0$, the amplitude of the characteristic localized field will be zero because of the influence of both the upper and lower bands. The singularity corresponding to the characteristic localized field in the radiation spectrum will vanish (as shown in Fig. 10).

When the upper level is within region II (or III), there are one propagating field with frequency being in the lower (or upper) band and the diffusion field in the radiation field. The peak of the diffusion field at frequency ω_{c_2} (ω_{c_1}) is very small as ω_1 in region II (III), and the other peak at frequency ω_{c_1} (ω_{c_2}) is covered by the large peak for the propagating field. So in the emission spectrum there is mainly one peak, which does not change for different distances from the atom r (See Fig. 11). When the upper level is within region IV (or V), only diffusion field exists, and the main peak occurs at

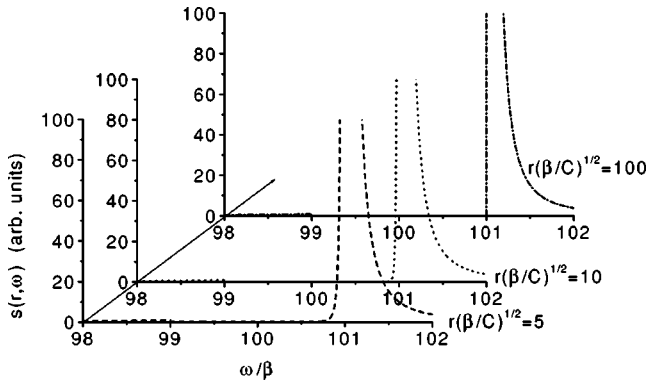

FIG. 12. The spectra of spontaneous emission from the excited atom for $\omega_{c_1}=101\beta$, $\omega_{c_2}=99\beta$, and $\omega_1=101.011507\beta$ (region V) with different distances from atom.

frequency ω_{c_2} (ω_{c_1}). When the distances from the atom r increases, the emission spectrum is narrowed due to drop of the emission spectrum within the band gap (as shown in Fig. 12).

VI. CONCLUSIONS

We have studied the properties of the spontaneous radiation from a two-level atom embedded in a three-dimensional anisotropic photonic crystal with an upper band, a lower band, and a band gap. It is found that the properties of the spontaneous emission and the emitted field are dependent strongly on the relative position of the upper level from the two bands (five regions). As a special cavity, a photonic crystal can affect the traveling behavior and the radiation spectrum. The faster and slower decay components corresponding to the diffusion field and the propagating field appear in the decay process for the emitted field. The radiation spectrum is more complex, and dependent on the location of the observer. We have also discussed the influence of the existence of the second band (the lower band) on spontaneous emission, Lamb shift, the emitted field and the radiation spectrum. The coexistence of the upper and lower bands leads to the stronger coupling between the atomic transition and the electromagnetic modes, and time evolution decay of the population in the excited state is faster than that in the single-band case. Due to different contributions of the upper band and the lower band, the Lamb shift becomes very small, the amplitude of the characteristic localized field may be zero, and the singularity caused by the localized field may vanish in the radiation spectrum.

ACKNOWLEDGMENTS

This work was supported in part by the National Natural Science Foundation of China, the 973 Project of Ministry of Science and Technology of China, Deutsche Forschungsgemeinschaft, and a RGC and CRGC from the Hong Kong Government. Y.Y. thanks the Humboldt Foundation for its generous support.

APPENDIX A: THE CALCULATION OF Γ

We can calculate Γ in Eq. (6) as follows:

$$\begin{aligned}\Gamma &= \sum_k \frac{g_k^2}{s+i(\omega_k-\omega_1)} \\ &= \frac{(\omega_1 d_1)^2}{2\epsilon_0\hbar V_0}\sum_k \frac{(\mathbf{e}_k\cdot\mathbf{u}_d)(\mathbf{e}_k\cdot\mathbf{u}_d)}{\omega_k[s+i(\omega_k-\omega_1)]} \\ &= \frac{(\omega_1 d_1)^2}{16\pi^3\epsilon_0\hbar}\int\int\int \frac{d^3\mathbf{k}}{\omega_k[s+i(\omega_k-\omega_1)]}\left[1-\frac{(\mathbf{k}\cdot\mathbf{u}_d)^2}{k^2}\right] \\ &= \frac{(\omega_1 d_1)^2}{16\pi^3\epsilon_0\hbar}\int\int\int^{\text{upper}} \frac{d^3\mathbf{k}}{\omega_k[s+i(\omega_k-\omega_1)]}\left[1-\frac{(\mathbf{k}\cdot\mathbf{u}_d)^2}{k^2}\right] \\ &\quad + \frac{(\omega_1 d_1)^2}{16\pi^3\epsilon_0\hbar}\int\int\int^{\text{lower}} \frac{d^3\mathbf{k}}{\omega_k[s+i(\omega_k-\omega_1)]} \\ &\quad \times\left[1-\frac{(\mathbf{k}\cdot\mathbf{u}_d)^2}{k^2}\right] \\ &= \Gamma_1+\Gamma_2, \end{aligned} \tag{A1}$$

where we have replaced the sum by an integral via $\Sigma_k \rightarrow [V_0/(2\pi)^3]\int\int\int d^3\mathbf{k}$, and

$$\begin{aligned}(\mathbf{e}_k\cdot\mathbf{u}_d)(\mathbf{e}_k\cdot\mathbf{u}_d) &= \mathbf{u}_d\cdot\mathbf{u}_d - \frac{(\mathbf{k}\cdot\mathbf{u}_d)\cdot(\mathbf{k}\cdot\mathbf{u}_d)}{k^2} \\ &= 1-\frac{(\mathbf{k}\cdot\mathbf{u}_d)\cdot(\mathbf{k}\cdot\mathbf{u}_d)}{k^2}.\end{aligned}$$

Due to the existence of the upper and lower bands, Γ can be written as the sum of two parts, Γ_1 and Γ_2. Near the upper (lower) band edge, the dispersion relation may be expressed approximately by $\omega_k=\omega_{c_1}+C_1|\mathbf{k}-\mathbf{k}_{10}^j|^2$ ($\omega_k=\omega_{c_2}-C_2|\mathbf{k}-\mathbf{k}_{20}^j|^2$). The integration over $\mathbf{k}$ has to be carried out around the direction of each $\mathbf{k}_{10}^j$ (or $\mathbf{k}_{20}^j$) because of the anisotropy of a three-dimensional photonic crystal. The angle between the dipole vector of the atom and the jth $\mathbf{k}_{10}^j$ ($\mathbf{k}_{20}^j$) is θ_j (φ_j). The angle between the dipole and $\mathbf{k}$ near $\mathbf{k}_{10}^j$ ($\mathbf{k}_{20}^j$) is replaced approximately by θ_j (φ_j). We can also extend the integration over $\mathbf{k}$ to infinity because the frequencies far away from the band edges do not contribute significantly. So we calculate Γ_1 and Γ_2 as follows:

$$\begin{aligned}\Gamma_1 &= \frac{(\omega_1 d_1)^2}{16\pi^3\epsilon_0\hbar}\int\int\int^{\text{upper}} \frac{d^3\mathbf{k}}{\omega_k[s+i(\omega_k-\omega_1)]}\left[1-\frac{(\mathbf{k}\cdot\mathbf{u}_d)^2}{k^2}\right] \\ &= \frac{(\omega_1 d_1)^2}{16\pi^3\epsilon_0\hbar}\left(\sum_j \sin^2\theta_j\right)\int\int\int_j^{\text{upper}} \frac{d^3\mathbf{q}}{(\omega_{c_1}+C_1|\mathbf{q}|^2)[s+i(\omega_{c_1}-\omega_1+C_1|\mathbf{q}|^2)]} \\ &= -\frac{(\omega_1 d_1)^2}{8\pi^2\epsilon_0\hbar C_1^{3/2}}\left(\sum_j \sin^2\theta_j\right)\frac{i}{\sqrt{\omega_{c_1}}+\sqrt{-is-(\omega_1-\omega_{c_1})}}\end{aligned} \tag{A2}$$

and

$$\Gamma_2=\frac{(\omega_1 d_1)^2}{16\pi^3\epsilon_0\hbar}\int\int\int^{\text{lower}}\frac{d^3\mathbf{k}}{\omega_k[s+i(\omega_k-\omega_1)]}\left[1-\frac{(\mathbf{k}\cdot\mathbf{u}_d)^2}{k^2}\right]$$

$$=\frac{(\omega_1 d_1)^2}{16\pi^3\epsilon_0\hbar}\left(\sum_j \sin^2\varphi_j\right)\int\int\int_j^{\text{lower}}\frac{d^3\mathbf{q}}{(\omega_{c_2}-C_2|\mathbf{q}|^2)[s+i(\omega_{c_2}-\omega_1-C_2|\mathbf{q}|^2)]}$$

$$\simeq\frac{(\omega_1 d_1)^2}{4\pi^2\epsilon_0\hbar}\left(\sum_j \sin^2\varphi_j\right)\int_0^\infty\frac{q^2dq}{(\omega_{c_2}+C_2q^2)[s+i(\omega_{c_2}-\omega_1-C_2q^2)]}=\frac{(\omega_1 d_1)^2}{8\pi^2\epsilon_0\hbar C_2^{3/2}}\left(\sum_j \sin^2\varphi_j\right)\frac{i}{\sqrt{\omega_{c_2}}+\sqrt{is+(\omega_1-\omega_{c_2})}}. \tag{A3}$$

Consequently, we have

$$\Gamma=-\frac{i\beta_1^{3/2}}{\sqrt{\omega_{c_1}}+\sqrt{-is-(\omega_1-\omega_{c_1})}}+\frac{i\beta_2^{3/2}}{\sqrt{\omega_{c_2}}+\sqrt{is+(\omega_1-\omega_{c_2})}} \tag{A4}$$

with $\beta_1^{3/2}=(\omega_1 d_1)^2\Sigma_j\sin^2\theta_j/(8\pi\epsilon_0\hbar C_1^{3/2})$ and $\beta_2^{3/2}=(\omega_1 d_1)^2\Sigma_j\sin^2\varphi_j/(8\pi\epsilon_0\hbar C_2^{3/2})$.

APPENDIX B: THE CALCULATION OF THE AMPLITUDES $A_1(T)$

For convenience in the following calculation, we define functions $G(x)$, $F(x)$, $K(x)$, $M(x)$, and $N(x)$ as follows:

$$G(x)=x-\frac{i}{\sqrt{\Omega_{c_1}}+\sqrt{-ix-(\Omega_1-\Omega_{c_1})}}+\frac{i}{\sqrt{\Omega_{c_2}}+\sqrt{ix+(\Omega_1-\Omega_{c_2})}}, \tag{B1}$$

$$F(x)=x-\frac{i}{\sqrt{\Omega_{c_1}}+\sqrt{-ix-(\Omega_1-\Omega_{c_1})}}+\frac{i}{\sqrt{\Omega_{c_2}}+i\sqrt{-ix-(\Omega_1-\Omega_{c_2})}}, \tag{B2}$$

$$K(x)=x-\frac{i}{\sqrt{\Omega_{c_1}}-\sqrt{ix+(\Omega_1-\Omega_{c_1})}}+\frac{i}{\sqrt{\Omega_{c_2}}+\sqrt{ix+(\Omega_1-\Omega_{c_2})}}, \tag{B3}$$

$$M(x)=-x+(\Omega_1-\Omega_{c_1})i+\frac{i}{\sqrt{\Omega_{c_2}}+\sqrt{-ix+(\Omega_{c_1}-\Omega_{c_2})}}, \tag{B4}$$

$$N(x)=-x+(\Omega_1-\Omega_{c_2})i-\frac{i}{\sqrt{\Omega_{c_1}}+\sqrt{ix+(\Omega_{c_1}-\Omega_{c_2})}}. \tag{B5}$$

where $\Omega_{c_1}=\omega_{c_1}/\beta$, $\Omega_{c_2}=\omega_{c_2}/\beta$, and $\Omega_1=\omega_1/\beta$. Using the inverse Laplace transform, the amplitude $A(t)$ can be written as

$$A_1(t)=\frac{1}{2\pi i}\int_{\sigma-i\infty}^{\sigma+i\infty}A_1(s)e^{st}ds=\sum_j\frac{e^{x_j^{(1)}\beta t}}{G'(x_j^{(1)})}-\frac{1}{2\pi i}\left[\int_{\infty i+0}^{(\Omega_1-\Omega_{c_2})i+0}+\int_{(\Omega_1-\Omega_{c_2})i}^{(\Omega_1-\Omega_{c_2})i-\infty}+\int_{(\Omega_1-\Omega_{c_1})i}^{(\Omega_1-\Omega_{c_1})i-\infty}+\int_{(\Omega_1-\Omega_{c_1})i+0}^{-\infty i+0}\right]\frac{1}{G(x)}e^{x\beta t}dx. \tag{B6}$$

Here $x_j^{(1)}$ are the roots of the equation $G(x)=0$ in region $[\mathrm{Re}(x)>0]$ or $[\Omega_1-\Omega_{c_1}<\mathrm{Im}(x)<\Omega_1-\Omega_{c_2}]$. The real number σ' is chosen so that $x=\sigma'$ lies to the right of all the singularity $x_j^{(1)}$. The integration contours for Eq. (B6) are shown in Fig. 13.

$$\frac{1}{2\pi i}\int_{\infty i+0}^{(\Omega_1-\Omega_{c_2})i+0}\frac{1}{G(x)}e^{x\beta t}dx=\frac{1}{2\pi i}\int_{\infty i}^{(\Omega_1-\Omega_{c_2})i}\frac{1}{x-\dfrac{i}{\sqrt{\Omega_{c_1}}+\sqrt{-ix-(\Omega_1-\Omega_{c_1})}}+\dfrac{i}{\sqrt{\Omega_{c_2}}+i\sqrt{-ix-(\Omega_1-\Omega_{c_2})}}}e^{x\beta t}dx$$

$$=-\sum_j\frac{e^{x_j^{(2)}\beta t}}{F'(x_j^{(2)})}$$

$$-\frac{1}{2\pi i}\int_0^{-\infty}\frac{e^{i(\omega_1-\omega_{c_2})t}e^{x\beta t}}{x+(\Omega_1-\Omega_{c_2})i-\dfrac{i}{\sqrt{\Omega_{c_1}}+\sqrt{-ix+(\Omega_{c_1}-\Omega_{c_2})}}+\dfrac{i}{\sqrt{\Omega_{c_2}}+i\sqrt{-ix}}}dx, \quad \text{(B7)}$$

$x_j^{(2)}$ are the roots of the equation $F(x)=0$ in region $[\mathrm{Re}(x)<0$ and $\mathrm{Im}(x)>(\Omega_1-\Omega_{c_2})]$. The integration contours for Eq. (B7) are shown in Fig. 14.

$$\frac{1}{2\pi i}\int_{(\Omega_1-\Omega_{c_2})i}^{(\Omega_1-\Omega_{c_2})i-\infty}\frac{1}{G(x)}e^{x\beta t}dx=\frac{1}{2\pi i}\int_0^{-\infty}\frac{e^{i(\omega_1-\omega_{c_2})t}e^{x\beta t}}{x+(\Omega_1-\Omega_{c_2})i-\dfrac{i}{\sqrt{\Omega_{c_1}}+\sqrt{-ix+(\Omega_{c_1}-\Omega_{c_2})}}+}\frac{i}{\sqrt{\Omega_{c_2}}+\sqrt{ix}}dx, \quad \text{(B8)}$$

$$\frac{1}{2\pi i}\int_{(\Omega_1-\Omega_{c_1})i}^{(\Omega_1-\Omega_{c_1})i-\infty}\frac{1}{G(x)}e^{x\beta t}dx=\frac{1}{2\pi i}\int_{-\infty}^{0}\frac{e^{i(\omega_1-\omega_{c_1})t}e^{x\beta t}}{x+(\Omega_1-\Omega_{c_1})i-\dfrac{i}{\sqrt{\Omega_{c_1}}+\sqrt{-ix}}+\dfrac{i}{\sqrt{\Omega_{c_2}}+\sqrt{ix+(\Omega_{c_1}-\Omega_{c_2})}}}dx, \quad \text{(B9)}$$

$$\frac{1}{2\pi i}\int_{(\Omega_1-\Omega_{c_1})i+0}^{-\infty i+0}\frac{1}{G(x)}e^{x\beta t}dx=\frac{1}{2\pi i}\int_{(\Omega_1-\Omega_{c_1})i}^{-\infty i}\frac{e^{x\beta t}}{x-\dfrac{i}{\sqrt{\Omega_{c_1}}-i\sqrt{ix+(\Omega_1-\Omega_{c_1})}}+\dfrac{i}{\sqrt{\Omega_{c_2}}+\sqrt{ix+(\Omega_1-\Omega_{c_2})}}}dx$$

$$=-\sum_j\frac{e^{x_j^{(3)}\beta t}}{K'(x_j^{(3)})}-\frac{1}{2\pi i}\int_{-\infty}^{0}\frac{e^{i(\omega_1-\omega_{c_1})t}e^{x\beta t}}{x+(\Omega_1-\Omega_{c_1})i-\dfrac{i}{\sqrt{\Omega_{c_1}}-i\sqrt{ix}}+\dfrac{i}{\sqrt{\Omega_{c_2}}+\sqrt{ix+(\Omega_{c_1}-\Omega_{c_2})}}}dx. \quad \text{(B10)}$$

In Eq. (B10), $x_j^{(3)}$ are the roots of $K(x)=0$ in region $[\mathrm{Re}(x)<0$ and $\mathrm{Im}(x)<(\Omega_1-\Omega_{c_1})]$. The integration contours for Eq. (B10) are shown in Fig. 15. Substituting Eqs. (B7)–(B10) into Eq. (B6), we get

$$A_1(t)=\sum_j\frac{e^{x_j^{(1)}\beta t}}{G'(x_j^{(1)})}+\sum_j\frac{e^{x_j^{(2)}\beta t}}{F'(x_j^{(2)})}+\sum_j\frac{e^{x_j^{(3)}\beta t}}{K'(x_j^{(3)})}+\frac{1}{2\pi i}\int_0^{\infty}\left[\frac{e^{i(\omega_1-\omega_{c_1})t}e^{-x\beta t}}{M(x)-\dfrac{i}{\sqrt{\Omega_{c_1}}-i\sqrt{-ix}}}-\frac{e^{i(\omega_1-\omega_{c_1})t}e^{-x\beta t}}{M(x)-\dfrac{i}{\sqrt{\Omega_{c_1}}+\sqrt{ix}}}\right]dx$$

$$-\frac{1}{2\pi i}\int_0^{\infty}\left[\frac{e^{i(\omega_1-\omega_{c_2})t}e^{-x\beta t}}{N(x)+\dfrac{i}{\sqrt{\Omega_{c_2}}+i\sqrt{ix}}}-\frac{e^{i(\omega_1-\omega_{c_2})t}e^{-x\beta t}}{N(x)+\dfrac{i}{\sqrt{\Omega_{c_2}}+\sqrt{-ix}}}\right]dx$$

$$=\sum_j\frac{e^{x_j^{(1)}\beta t}}{G'(x_j^{(1)})}+\sum_j\frac{e^{x_j^{(2)}\beta t}}{F'(x_j^{(2)})}+\sum_j\frac{e^{x_j^{(3)}\beta t}}{K'(x_j^{(3)})}+\frac{1}{\pi}\int_0^{\infty}\left[\frac{i^{1/2}\sqrt{x}e^{i(\omega_1-\omega_{c_1})t}}{(M(x)\sqrt{\Omega_{c_1}}-i)^2-iM^2(x)x}\right.$$

$$\left.+\frac{i^{-1/2}\sqrt{x}e^{i(\omega_1-\omega_{c_2})t}}{(N(x)\sqrt{\Omega_{c_2}}+i)^2+iN^2(x)x}\right]e^{-x\beta t}dx. \quad \text{(B11)}$$

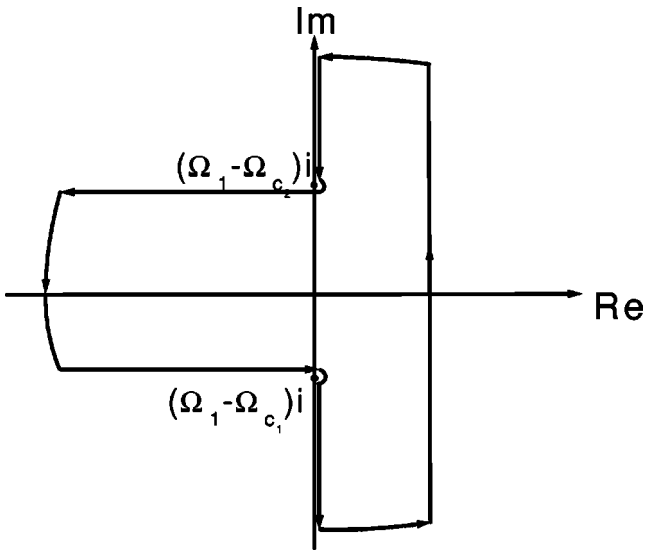

FIG. 13. The integration contours for Eq. (B6).

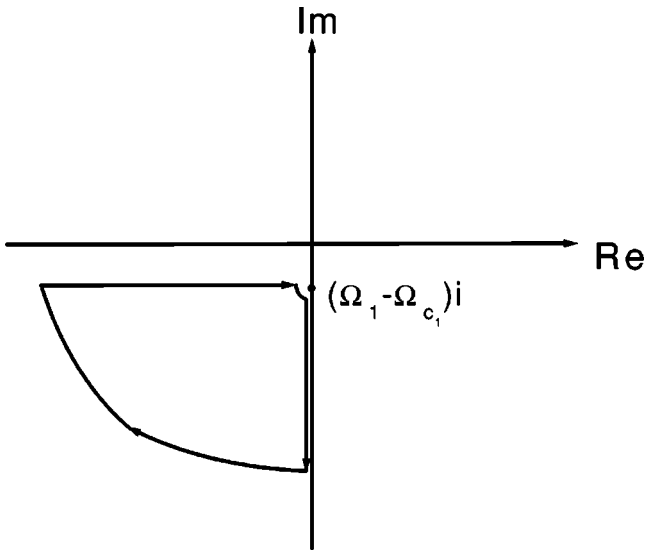

FIG. 15. The integration contours for Eq. (B10).

APPENDIX C: PROOF OF THE ROOT FOR $G(x)=0$

1. Purely imaginary root for $G(x)=0$ in the region $\Omega_1-\Omega_{c_1}<\mathrm{Im}(x)<\Omega_1-\Omega_{c_2}$

Here we only discuss the purely imaginary root for the following equation:

$$x-\frac{i}{\sqrt{\Omega_{c_1}}+\sqrt{-ix-(\Omega_1-\Omega_{c_1})}}+\frac{i}{\sqrt{\Omega_{c_2}}+\sqrt{ix+(\Omega_1-\Omega_{c_2})}}=0. \tag{C1}$$

If we set $x=iy$ (y is a real number), the above equation becomes

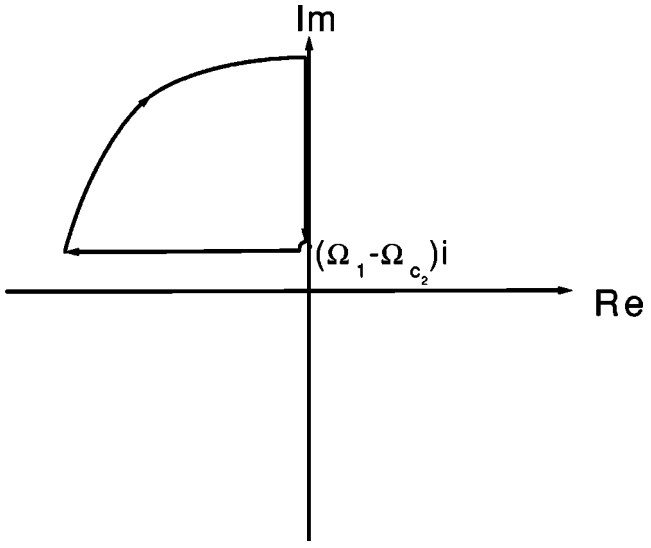

FIG. 14. The integration contours for Eq. (B7).

$$y-\frac{1}{\sqrt{\Omega_{c_1}}+\sqrt{y-(\Omega_1-\Omega_{c_1})}}+\frac{1}{\sqrt{\Omega_{c_2}}+\sqrt{-y+(\Omega_1-\Omega_{c_2})}}=0. \tag{C2}$$

Obviously, there are no real roots for Eq. (C2) in regions $(-\infty,\ \Omega_1-\Omega_{c_1})$ and $(\Omega_1-\Omega_{c_2},\ \infty)$. In region $(\Omega_1-\Omega_{c_1},\ \Omega_1-\Omega_{c_2})$, we define the following function:

$$f(y)=y-\frac{1}{\sqrt{\Omega_{c_1}}+\sqrt{y-(\Omega_1-\Omega_{c_1})}}+\frac{1}{\sqrt{\Omega_{c_2}}+\sqrt{-y+(\Omega_1-\Omega_{c_2})}}. \tag{C3}$$

We can obtain

$$f'(y)>0, \tag{C4}$$

$$f(y)|_{y\to\Omega_1-\Omega_{c_1}}=\Omega_1-\Omega_{c_1}-\frac{1}{\sqrt{\Omega_{c_1}}}+\frac{1}{\sqrt{\Omega_{c_2}}+\sqrt{\Omega_{c_1}-\Omega_{c_2}}}, \tag{C5}$$

$$f(y)|_{y\to\Omega_1-\Omega_{c_2}}=\Omega_1-\Omega_{c_2}-\frac{1}{\sqrt{\Omega_{c_1}}+\sqrt{\Omega_{c_1}-\Omega_{c_2}}}+\frac{1}{\sqrt{\Omega_{c_2}}}. \tag{C6}$$

Only when $f(y)|_{y\to\Omega_1-\Omega_{c_1}}\leqslant 0$ and $f(y)|_{y\to\Omega_1-\Omega_{c_2}}\geqslant 0$ is there only one real root of the equation $f(y)=0$. That is to say, there is only one purely imaginary root in region $\Omega_1-\Omega_{c_1}\leqslant\mathrm{Im}(x)\leqslant\Omega_1-\Omega_{c_2}$ for $G(x)=0$ as $\Omega_{c_2}+[1/(\sqrt{\Omega_{c_1}}+\sqrt{\Omega_{c_1}-\Omega_{c_2}})]-(1/\sqrt{\Omega_{c_2}})\leqslant\Omega_1\leqslant\Omega_{c_1}+(1/\sqrt{\Omega_{c_1}})-[1/(\sqrt{\Omega_{c_2}}+\sqrt{\Omega_{c_1}-\Omega_{c_2}})]$.

2. No complex root with $\mathrm{Re}(x)\neq 0$ for $G(x)=0$ in the region $[\Omega_1-\Omega_{c_1}<\mathrm{Im}(x)<\Omega_1-\Omega_{c_2}$ or $\mathrm{Re}(x)>0]$

Suppose $x=a+ib$ with $a\neq 0$ is the complex root of $G(x)=0$. We can analyze the root as follows:

(1) If $a>0$, we can obtain the regions for the phase angles, $-\pi/2<\arg[\sqrt{\Omega_{c_1}}+\sqrt{-ix-(\Omega_1-\Omega_{c_1})}]<0$ and $0<\arg[\sqrt{\Omega_{c_2}}+\sqrt{ix+(\Omega_1-\Omega_{c_2})}]<\pi/2$. Then we have

$$\frac{\pi}{2}<\arg\left(\frac{i}{\sqrt{\Omega_{c_1}}+\sqrt{-ix-(\Omega_1-\Omega_{c_1})}}\right)<\pi, \tag{C7}$$

$$0<\arg\left(\frac{i}{\sqrt{\Omega_{c_2}}+\sqrt{ix+(\Omega_1-\Omega_{c_2})}}\right)<\frac{\pi}{2}. \tag{C8}$$

From the equation $G(x)=0$, we get $x=[i/(\sqrt{\Omega_{c_1}}+\sqrt{-ix-(\Omega_1-\Omega_{c_1})})]-[i/(\sqrt{\Omega_{c_2}}+\sqrt{ix+(\Omega_1-\Omega_{c_2})})]$. From Eqs. (C7) and (C8) we know that $\mathrm{Re}\{[i/(\sqrt{\Omega_{c_1}}+\sqrt{-ix-(\Omega_1-\Omega_{c_1})})]-[i/\sqrt{\Omega_{c_2}}+\sqrt{ix+(\Omega_1-\Omega_{c_2})}]\}<0$, which disagrees with the above supposition $a>0$. So $x=a+ib$ with $a>0$ is not the root of $G(x)=0$.

(2) If $a<0$ and $\Omega_1-\Omega_{c_1}<b<\Omega_1-\Omega_{c_2}$, we have $0<\arg[\sqrt{\Omega_{c_1}}+\sqrt{-ix-(\Omega_1-\Omega_{c_1})}]<\pi/4$ and $-\pi/4<\arg[\sqrt{\Omega_{c_2}}+\sqrt{ix+(\Omega_1-\Omega_{c_2})}]<0$.

$$\frac{\pi}{4}<\arg\left(\frac{i}{\sqrt{\Omega_{c_1}}+\sqrt{-ix-(\Omega_1-\Omega_{c_1})}}\right)<\frac{\pi}{2}, \tag{C9}$$

$$\frac{\pi}{2}<\arg\left(\frac{i}{\sqrt{\Omega_{c_2}}+\sqrt{ix+(\Omega_1-\Omega_{c_2})}}\right)<\pi. \tag{C10}$$

From Eqs. (C9) and (C10) we obtain $\mathrm{Re}(x)=\mathrm{Re}\{[i/\sqrt{\Omega_{c_1}}+\sqrt{-ix-(\Omega_1-\Omega_{c_1})}]-[i/\sqrt{\Omega_{c_2}}+\sqrt{ix+(\Omega_1-\Omega_{c_2})}]\}>0$. It does not agree with the supposition $a<0$. So $x=a+ib$ with $a<0$ is not the complex root of $G(x)=0$ in the region $\Omega_1-\Omega_{c_1}<\mathrm{Im}(x)<\Omega_1-\Omega_{c_2}$.

From the above discussions, we can see that there are no complex roots with $\mathrm{Re}(x)\neq 0$ for $G(x)=0$ in the region $[\Omega_1-\Omega_{c_1}<\mathrm{Im}(x)<\Omega_1-\Omega_{c_2}$ or $\mathrm{Re}(x)>0]$.

APPENDIX D: THE CALCULATION OF THE RADIATION FIELD $E(R,T)$

The amplitude of the radiated field at a particular space point $\mathbf{r}$ [14] is

$$\begin{aligned}\mathbf{E}(\mathbf{r},t)&=\sum_k\sqrt{\frac{\hbar\omega_k}{2\varepsilon_0 V_0}}e^{-i(\omega t-\mathbf{k}\cdot\mathbf{r})}B_k(t)\mathbf{e}_k\\&=\sum_k\frac{\omega_1 d_1}{2\varepsilon_0 V_0}e^{-i(\omega t-\mathbf{k}\cdot\mathbf{r})}\left[\int_0^t A(t')e^{i(\omega_k-\omega_1)t'}dt'\right]\\&\quad\times\left[\mathbf{u}_d-\frac{\mathbf{k}(\mathbf{k}\cdot\mathbf{u}_d)}{k^2}\right]\\&=\sum_{j,k_1(j)}\frac{\omega_1 d_1}{2\varepsilon_0 V_0}e^{-i(\omega t-\mathbf{k}_{10}^j\cdot\mathbf{r}-\mathbf{q}_1\cdot\mathbf{r})}\\&\quad\times\left[\int_0^t A(t')e^{i(\omega_{q_1}-\omega_1)t'}dt'\right]\left[\mathbf{u}_d-\frac{\mathbf{k}_{10}^j(\mathbf{k}_{10}^j\cdot\mathbf{u}_d)}{(k_{10}^j)^2}\right]\\&\quad+\sum_{j,k_2(j)}\frac{\omega_1 d_1}{2\varepsilon_0 V_0}e^{-i(\omega t-\mathbf{k}_{20}^j\cdot\mathbf{r}-\mathbf{q}_2\cdot\mathbf{r})}\\&\quad\times\left[\int_0^t A(t')e^{i(\omega_{q_2}-\omega_1)t'}dt'\right]\left[\mathbf{u}_d-\frac{\mathbf{k}_{20}^j(\mathbf{k}_{20}^j\cdot\mathbf{u}_d)}{(k_{20}^j)^2}\right]\\&=\frac{\omega_1 d_1}{16\pi^3\varepsilon_0}\sum_j e^{i\mathbf{k}_{10}^j\cdot\mathbf{r}}\left[\mathbf{u}_d-\frac{\mathbf{k}_{10}^j(\mathbf{k}_{10}^j\cdot\mathbf{u}_d)}{(k_{10}^j)^2}\right]\\&\quad\times\int\int\int d^3\mathbf{q}_1 e^{-i(\omega_{q_1}t-\mathbf{q}_1\cdot\mathbf{r})}\\&\quad\times\left[\int_0^t A(t')e^{i(\omega_{q_1}-\omega_1)t'}dt'\right]+\frac{\omega_1 d_1}{16\pi^3\varepsilon_0}\sum_j e^{i\mathbf{k}_{20}^j\cdot\mathbf{r}}\\&\quad\times\left[\mathbf{u}_d-\frac{\mathbf{k}_{20}^j(\mathbf{k}_{20}^j\cdot\mathbf{u}_d)}{(k_{20}^j)^2}\right]\int\int\int d^3\mathbf{q}_2 e^{-i(\omega_{q_2}t-\mathbf{q}_2\cdot\mathbf{r})}\\&\quad\times\left[\int_0^t A(t')e^{i(\omega_{q_2}-\omega_1)t'}dt'\right].\end{aligned} \tag{D1}$$

Here $q_1=\mathbf{k}-\mathbf{k}_{10}^i$ and $q_2=\mathbf{k}-\mathbf{k}_{20}^j$. The sum over $\mathbf{k}$ is composed of two parts, which are for the upper and lower bands, respectively. Due to anisotropy, the sum over $\mathbf{k}_1$ ($\mathbf{k}_2$) for the upper (lower) band has to be carried out around the direction of each $\mathbf{k}_{10}^j$ ($\mathbf{k}_{20}^j$). We have also replaced the sum over $\mathbf{k}_1$ (or $\mathbf{k}_2$) by integration.

Suppose $A(t')=e^{x\beta t'}$, we have

$$\begin{aligned}&\int\int\int d^3\mathbf{q}_1 e^{-i(\omega_{q_1}t-\mathbf{q}_1\cdot\mathbf{r})}\left[\int_0^t A(t')e^{i(\omega_{q_1}-\omega_1)t'}dt'\right]\\&=\int\int\int d^3\mathbf{q}_1\frac{e^{(x\beta-i\omega_1)t+i\mathbf{q}_1\cdot\mathbf{r}}-e^{-i(\omega_{q_1}t-\mathbf{q}_1\cdot\mathbf{r})}}{i(\omega_{q_1}-\omega_1)+x\beta}\\&=\frac{2\pi}{ir}\int_{-\infty}^{\infty}\frac{e^{(x\beta-i\omega_1)t}-e^{-i\omega_{q_1}t}}{i(\omega_{q_1}-\omega_1)+x\beta}e^{iq_1 r}q_1 dq_1,\end{aligned} \tag{D2}$$

$$\int_{-\infty}^{\infty}\frac{e^{(x\beta-i\omega_1)t}}{i(\omega_{q_1}-\omega_1)+x\beta}e^{iq_1 r}q_1 dq_1$$

$$=\frac{\pi}{C_1}e^{(x\beta-i\omega_1)t-r\sqrt{((\omega_{c_1}-\omega_1)-ix\beta)/C_1}}, \tag{D3}$$

$$\int_{-\infty}^{\infty}\frac{e^{-i\omega_{q_1}t}}{i(\omega_{q_1}-\omega_1)+x\beta}e^{iq_1 r}q_1 dq_1$$

$$=\int_{-\infty}^{\infty}\frac{\left(q+\frac{r}{2C_1 t}\right)e^{-iC_1 tq^2}e^{-i[\omega_{c_1}t-(r^2/4C_1 t)]}}{i(\omega_{c_1}-\omega_1)+iC_1\left(q+\frac{r}{2C_1 t}\right)^2+x\beta}dq, \tag{D4}$$

with

$$\int_{-\infty}^{0}\frac{\left(q+\frac{r}{2C_1t}\right)e^{-iC_1tq^2}e^{-i(\omega_{c_1}t-r^2/4C_1t)}}{i(\omega_{c_1}-\omega_1)+iC_1\left(q+\frac{r}{2C_1t}\right)^2+x\beta}dq=\frac{\pi}{C_1}e^{(x\beta-i\omega_1)t-r\sqrt{[(\omega_{c_1}-\omega_1)-ix\beta]/C_1}}$$

$$\times\begin{cases}1 & [\mathrm{Im}(x\beta)<\omega_1-\omega_{c_1}]\\ \Theta[r+2t\sqrt{C_1}(\mathrm{Im}-\mathrm{Re})\sqrt{\omega_{c_1}-\omega_1-ix\beta}] & [\mathrm{Im}(x\beta)\geqslant\omega_1-\omega_{c_1}]\end{cases}$$

$$-e^{-i[\omega_{c_1}t-(r^2/4C_1t]+(3/4)\pi i}\int_0^{\infty}\frac{\left(\rho e^{(3/4)\pi i}+\frac{r}{2C_1t}\right)e^{-C_1t\rho^2}}{x\beta+i(\omega_{c_1}-\omega_1)+iC_1\left(\rho e^{(3/4)\pi i}+\frac{r}{2C_1t}\right)^2}d\rho$$

and

$$\int_0^{\infty}\frac{\left(q+\frac{r}{2C_1t}\right)e^{-iC_1tq^2}e^{-i[\omega_{c_1}t-(r^2/4C_1t)]}}{i(\omega_{c_1}-\omega_1)+iC_1\left(q+\frac{r}{2C_1t}\right)^2+x\beta}dq=-\frac{\pi}{C_1}e^{(x\beta-i\omega_1)t+r\sqrt{[(\omega_{c_1}-\omega_1)-ix\beta]/C_1}}$$

$$\times\begin{cases}\Theta[2t\sqrt{C_1}(\mathrm{Im}-\mathrm{Re})\sqrt{\omega_{c_1}-\omega_1-ix\beta}-r] & [\mathrm{Im}(x\beta)<\omega_1-\omega_{c_1}]\\ 0 & [\mathrm{Im}(x\beta)\geqslant\omega_1-\omega_{c_1}]\end{cases}$$

$$+e^{-i[\omega_{c_1}t-(r^2/4C_1t)]-1/4\pi i}\int_0^{\infty}\frac{\left(\rho e^{-(1/4)\pi i}+\frac{r}{2C_1t}\right)e^{-C_1t\rho^2}}{x\beta+i(\omega_{c_1}-\omega_1)+iC_1\left(\rho e^{-(1/4)\pi i}+\frac{r}{2C_1t}\right)^2}d\rho.$$

Here $\Theta(x)$ is the step function for $x\geqslant 0,\Theta(x)=1$, and $x<0,\Theta(x)=0$. So we can obtain

$$\frac{\omega_1 d_1}{16\pi^3\varepsilon_0}\sum_j e^{i\mathbf{k}_{10}^j\cdot\mathbf{r}}\left[\mathbf{u}_d-\frac{\mathbf{k}_{10}^j(\mathbf{k}_{10}^j\cdot\mathbf{u}_d)}{(k_{10}^j)^2}\right]\int\int\int d^3\mathbf{q}_1 e^{-i(\omega_{q_1}t-\mathbf{q}_1\cdot\mathbf{r})}\left[\int_0^t A(t')e^{i(\omega_{q_1}-\omega_1)t'}dt'\right]$$

$$=\frac{\omega_1 d_1}{8\pi^2\varepsilon_0 ri}\sum_j e^{i\mathbf{k}_{10}^j\cdot\mathbf{r}}\left[\mathbf{u}_d-\frac{\mathbf{k}_{10}^j(\mathbf{k}_{10}^j\cdot\mathbf{u}_d)}{(k_{10}^j)^2}\right]\int_{-\infty}^{\infty}\frac{e^{(x\beta-i\omega_1)t}-e^{-i\omega_{q_1}t}}{i(\omega_{q_1}-\omega_1)+x\beta}e^{iq_1r}q_1dq_1$$

$$=\frac{\omega_1 d_1}{8\pi^2\varepsilon_0 ri}\sum_j e^{i\mathbf{k}_{10}^j\cdot\mathbf{r}}\left[\mathbf{u}_d-\frac{\mathbf{k}_{10}^j(\mathbf{k}_{10}^j\cdot\mathbf{u}_d)}{(k_{10}^j)^2}\right]\Bigg\{\frac{\pi}{C_1}e^{(x\beta-i\omega_1)t-r\sqrt{[(\omega_{c_1}-\omega_1)-ix\beta]/C_1}}$$

$$\times\Theta[2t\sqrt{C_1}(\mathrm{Re}-\mathrm{Im})\sqrt{\omega_{c_1}-\omega_1-ix\beta}-r]\Theta[\omega_{c_1}-\omega_1+\mathrm{Im}(x\beta)]+\frac{\pi}{C_1}e^{(x\beta-i\omega_1)t+r\sqrt{[(\omega_{c_1}-\omega_1)-ix\beta]/C_1}}$$

$$\times\Theta[2t\sqrt{C_1}(\mathrm{Im}-\mathrm{Re})\sqrt{\omega_{c_1}-\omega_1-ix\beta}-r]\Theta[\omega_1-\omega_{c_1}-\mathrm{Im}(x\beta)]+e^{-i[\omega_{c_1}t-(r^2/4C_1t)]+(3/4)\pi i}$$

$$\times\int_{-\infty}^{\infty}\frac{\left(\rho e^{(3/4)\pi i}+\frac{r}{2C_1t}\right)e^{-C_1t\rho^2}}{x\beta+i(\omega_{c_1}-\omega_1)+iC_1\left(\rho e^{(3/4)\pi i}+\frac{r}{2C_1t}\right)^2}d\rho\Bigg\}. \tag{D5}$$

Similarly, we get

$$\int\int\int d^3\mathbf{q}_2 e^{-i(\omega_{q_2}t-\mathbf{q}_2\cdot\mathbf{r})}\left[\int_0^t A(t')e^{i(\omega_{q_2}-\omega_1)t'}dt'\right]=\frac{2\pi}{ir}\int_{-\infty}^{\infty}\frac{e^{(x\beta-i\omega_1)t}-e^{-i\omega_{q_2}t}}{i(\omega_{q_2}-\omega_1)+x\beta}e^{iq_2r}q_2dq_2, \tag{D6}$$

$$\int_{-\infty}^{\infty}\frac{e^{(x\beta-i\omega_1)t}}{i(\omega_{q_2}-\omega_1)+x\beta}e^{iq_2r}q_2dq_2=-\frac{\pi}{C_2}e^{(x\beta-i\omega_1)t-r\sqrt{[(\omega_1-\omega_{c_2})+ix\beta]/C_2}}, \tag{D7}$$

and

$$\begin{aligned}\int_{-\infty}^{\infty}\frac{e^{-i\omega_{q_2}t}}{i(\omega_{q_2}-\omega_1)+x\beta}e^{iq_2r}q_2dq_2&=\int_{-\infty}^{\infty}\frac{e^{-i(\omega_{c_2}-C_2q_2^2)t+iq_2r}q_2}{i(\omega_{c_2}-\omega_1-C_2q_2^2)+x\beta}dq_2\\&=-\frac{\pi}{C_1}e^{(x\beta-i\omega_1)t+r\sqrt{[(\omega_1-\omega_{c_2})+ix\beta]/C_2}}\Theta[-r-2t\sqrt{C_2}(\mathrm{Im}+\mathrm{Re})\sqrt{\omega_1-\omega_{c_2}+ix\beta}]\\&\times\Theta[\omega_{c_2}-\omega_1+\mathrm{Im}(x\beta)]-\frac{\pi}{C_1}e^{(x\beta-i\omega_1)t-r\sqrt{[(\omega_1-\omega_{c_2})+ix\beta]/C_2}}\Theta\\&\times[r-2t\sqrt{C_2}(\mathrm{Im}+\mathrm{Re})\sqrt{\omega_1-\omega_{c_2}+ix\beta}]\Theta[\omega_1-\omega_{c_2}-\mathrm{Im}(x\beta)]\\&-\frac{\pi}{C_1}e^{(x\beta-i\omega_1)t-r\sqrt{[(\omega_1-\omega_{c_2})+ix\beta]/C_2}}\Theta[\omega_{c_2}-\omega_1+\mathrm{Im}(x\beta)]-e^{-i[\omega_{c_2}t+(r^2/4C_2t)]-(3/4)\pi i}\\&\times\int_{-\infty}^{\infty}\frac{\left(\rho e^{-(3/4)\pi i}-\dfrac{r}{2C_2t}\right)e^{-C_2t\rho^2}}{x\beta+i(\omega_{c_2}-\omega_1)-iC_2\left(\rho e^{-(3/4)\pi i}-\dfrac{r}{2C_2t}\right)^2}d\rho.\end{aligned} \tag{D8}$$

So we have

$$\begin{aligned}&\frac{\omega_1 d_1}{16\pi^3\varepsilon_0}\sum_j e^{i\mathbf{k}_{20}^j\cdot\mathbf{r}}\left[\mathbf{u}_d-\frac{\mathbf{k}_{20}^j(\mathbf{k}_{20}^j\cdot\mathbf{u}_d)}{(k_{20}^j)^2}\right]\int\int\int d^3q_2 e^{-i(\omega_{q_2}t-\mathbf{q}_2\cdot\mathbf{r})}\left[\int_0^t A(t')e^{i(\omega_{q_2}-\omega_1)t'}dt'\right]\\&=\frac{\omega_1 d_1}{8\pi^2\varepsilon_0 ri}\sum_j e^{i\mathbf{k}_{20}^j\cdot\mathbf{r}}\left[\mathbf{u}_d-\frac{\mathbf{k}_{20}^j(\mathbf{k}_{20}^j\cdot\mathbf{u}_d)}{(k_{20}^j)^2}\right]\Bigg\{-\frac{\pi}{C_2}e^{(x\beta-i\omega_1)t-r\sqrt{[(\omega_1-\omega_{c_2})+ix\beta]/C_2}}\Theta\\&\times[2t\sqrt{C_2}(\mathrm{Re}+\mathrm{Im})\sqrt{\omega_1-\omega_{c_2}+ix\beta}-r]\Theta[\omega_1-\omega_{c_2}-\mathrm{Im}(x\beta)]+\frac{\pi}{C_2}e^{(x\beta-i\omega_1)t+r\sqrt{[(\omega_1-\omega_{c_2})+ix\beta]/C_2}}\Theta\\&\times[-2t\sqrt{C_2}(\mathrm{Im}+\mathrm{Re})\sqrt{\omega_1-\omega_{c_2}+ix\beta}-r]\Theta[\omega_{c_2}-\omega_1+\mathrm{Im}(x\beta)]+e^{-i[\omega_{c_2}t+(r^2/4C_2t)]-(3/4)\pi i}\\&\times\int_{-\infty}^{\infty}\frac{\left(\rho e^{-(3/4)\pi i}-\dfrac{r}{2C_2t}\right)e^{-C_2t\rho^2}}{x\beta+i(\omega_{c_2}-\omega_1)-iC_2\left(\rho e^{-(3/4)\pi i}-\dfrac{r}{2C_2t}\right)^2}d\rho\Bigg\}.\end{aligned} \tag{D9}$$

From Eqs. (B11), (D1), (D5), and (D9), we can calculate the radiation field $\mathbf{E}(\mathbf{r},t)$. Corresponding to each term in $A(t)$, we can obtain

$$\mathbf{E}(\mathbf{r},t)=\mathbf{E}^{(1)}(\mathbf{r},t)+\mathbf{E}^{(2)}(\mathbf{r},t)+\mathbf{E}^{(3)}(\mathbf{r},t)+\mathbf{E}^{(4)}(\mathbf{r},t). \tag{D10}$$

(1) For the pure imaginary root $x^{(1)}=ib^{(1)}/\beta$, we have $\omega_{c_2}<\omega_1-b^{(1)}<\omega_{c_1}$. The term in $A(t)$ related to $x^{(1)}$ is $e^{x_j^{(1)}\beta t}/G'(x_j^{(1)})$. So the term $\mathbf{E}^{(1)}(\mathbf{r},t)$ in the radiation field $\mathbf{E}(\mathbf{r},t)$ can be obtained as follows:

$$\mathbf{E}^{(1)}(\mathbf{r},t)=\frac{1}{G'(x^{(1)})}[\mathbf{E}_{10}(\mathbf{r})E_1^{(1)}(r,t)+\mathbf{E}_{20}(\mathbf{r})E_2^{(1)}(r,t)], \tag{D11}$$

with

$$E_1^{(1)}(r,t)=\frac{\pi}{C_1}e^{-i(\omega_1-b^{(1)})t-r\sqrt{(\omega_{c_1}-\omega_1+b^{(1)})/C_1}}\Theta\left(t-\frac{r}{2\sqrt{C_1}\sqrt{\omega_{c_1}-\omega_1+b^{(1)}}}\right)$$
$$+e^{-i[\omega_{c_1}t-(r^2/4C_1t)]+(1/4)\pi i}\int_{-\infty}^{\infty}\frac{\left(\rho e^{(3/4)\pi i}+\frac{r}{2C_1t}\right)e^{-C_1t\rho^2}}{(\omega_{c_1}-\omega_1+b^{(1)})+C_1\left(\rho e^{(3/4)\pi i}+\frac{r}{2C_1t}\right)^2}d\rho,$$

$$E_2^{(1)}(r,t)=-\frac{\pi}{C_2}e^{-i(\omega_1-b^{(1)})t-r\sqrt{(\omega_1-\omega_{c_2}-b^{(1)})/C_2}}\Theta\left(t-\frac{r}{2\sqrt{C_2}\sqrt{\omega_1-\omega_{c_2}-b^{(1)}}}\right)$$
$$+e^{-i[\omega_{c_2}t+(r^2/4C_2t)]-(1/4)\pi i}\int_{-\infty}^{\infty}\frac{\left(\rho e^{-(3/4)\pi i}-\frac{r}{2C_2t}\right)e^{-C_2t\rho^2}}{(\omega_1-b^{(1)}-\omega_{c_2})+C_2\left(\rho e^{-(3/4)\pi i}-\frac{r}{2C_2t}\right)^2}d\rho.$$

Here $\mathbf{E}_{10}(\mathbf{r})=(\omega_1 d_1/8\pi^2\varepsilon_0 ri)\Sigma_j e^{i\mathbf{k}_{10}^j\cdot\mathbf{r}}\{\mathbf{u}_d-[\mathbf{k}_{10}^j(\mathbf{k}_{10}^j\cdot\mathbf{u}_d)/(k_{10}^j)^2]\}$ and $\mathbf{E}_{20}(\mathbf{r})=(\omega_1 d_1/8\pi^2\varepsilon_0 ri)\Sigma_j e^{i\mathbf{k}_{20}^j\cdot\mathbf{r}}\{\mathbf{u}_d-[\mathbf{k}_{20}^j(\mathbf{k}_{20}^j\cdot\mathbf{u}_d)/(k_{20}^j)^2]\}$.

(2) For the complex root $x^{(2)}=(a^{(2)}+ib^{(2)})/\beta$, we have $\omega_1-b^{(2)}<\omega_{c_2}$ and $a^{(2)}<0$. The term $e^{x_j^{(2)}\beta t}/F'(x_j^{(2)})$ in $A(t)$ is related to $x^{(2)}$. So the term $\mathbf{E}^{(2)}(\mathbf{r},t)$ in the radiation field $\mathbf{E}(\mathbf{r},t)$ can be written as

$$\mathbf{E}^{(2)}(\mathbf{r},t)=\frac{1}{F'(x^{(2)})}[\mathbf{E}_{10}(\mathbf{r})E_1^{(2)}(r,t)+\mathbf{E}_{20}(\mathbf{r})E_2^{(2)}(r,t)], \tag{D12}$$

with

$$E_1^{(2)}(r,t)=\frac{\pi}{C_1}e^{-i(\omega_1+ix^{(2)}\beta)t-r\sqrt{(\omega_{c_1}-\omega_1-ix^{(2)}\beta)/C_1}}\Theta\left(t-\frac{r}{2\sqrt{C_1}(\mathrm{Re}-\mathrm{Im})\sqrt{\omega_{c_1}-\omega_1-ix^{(2)}\beta}}\right)$$
$$+e^{-i[\omega_{c_1}t-(r^2/4C_1t)]+(1/4)\pi i}\int_{-\infty}^{\infty}\frac{\left(\rho e^{(3/4)\pi i}+\frac{r}{2C_1t}\right)e^{-C_1t\rho^2}}{(\omega_{c_1}-\omega_1-ix^{(2)}\beta)+C_1\left(\rho e^{(3/4)\pi i}+\frac{r}{2C_1t}\right)^2}d\rho,$$

$$E_2^{(2)}(r,t)=\frac{\pi}{C_2}e^{-i(\omega_1+ix^{(2)}\beta)t+r\sqrt{(\omega_1-\omega_{c_2}+ix^{(2)}\beta)/C_2}}\Theta\left(t+\frac{r}{2\sqrt{C_2}(\mathrm{Re}+\mathrm{Im})\sqrt{\omega_1-\omega_{c_2}+ix^{(2)}\beta}}\right)$$
$$+e^{-i[\omega_{c_2}t+(r^2/4C_2t)]-(1/4)\pi i}\int_{-\infty}^{\infty}\frac{\left(\rho e^{-(3/4)\pi i}-\frac{r}{2C_2t}\right)e^{-C_2t\rho^2}}{(\omega_1+ix^{(2)}\beta-\omega_{c_2})+C_2\left(\rho e^{-(3/4)\pi i}-\frac{r}{2C_2t}\right)^2}d\rho.$$

(3) For the complex root $x^{(3)}=(a^{(3)}+ib^{(3)})/\beta$, we have $\omega_1-b^{(3)}>\omega_{c_1}$, and $a^{(2)}<0$. We can get $\mathbf{E}^{(3)}(\mathbf{r},t)$ in the radiation field $\mathbf{E}(\mathbf{r},t)$,

$$\mathbf{E}^{(3)}(\mathbf{r},t)=\frac{1}{K'(x^{(3)})}[\mathbf{E}_{10}(\mathbf{r})E_1^{(3)}(r,t)+\mathbf{E}_{20}(\mathbf{r})E_2^{(3)}(r,t)], \tag{D13}$$

with

$$E_1^{(3)}(r,t)=\frac{\pi}{C_1}e^{-i(\omega_1+ix^{(3)}\beta)t+r\sqrt{(\omega_{c_1}-\omega_1-ix^{(3)}\beta)/C_1}}\Theta\left(t-\frac{r}{2\sqrt{C_1}(\mathrm{Im}-\mathrm{Re})\sqrt{\omega_{c_1}-\omega_1-ix^{(3)}\beta}}\right)$$
$$+e^{-i[\omega_{c_1}t-(r^2/4C_1t)]+(1/4)\pi i}\int_{-\infty}^{\infty}\frac{\left(\rho e^{(3/4)\pi i}+\frac{r}{2C_1t}\right)e^{-C_1t\rho^2}}{(\omega_{c_1}-\omega_1-ix^{(3)}\beta)+C_1\left(\rho e^{(3/4)\pi i}+\frac{r}{2C_1t}\right)^2}d\rho,$$

$$E_2^{(3)}(r,t)=-\frac{\pi}{C_2}e^{-i(\omega_1+ix^{(3)}\beta)t-r\sqrt{(\omega_1-\omega_{c_2}+ix^{(2)}\beta)/C_2}}\Theta\left(t-\frac{r}{2\sqrt{C_2}(\mathrm{Re}+\mathrm{Im})\sqrt{\omega_1-\omega_{c_2}+ix^{(3)}\beta}}\right)$$
$$+e^{-i[\omega_{c_2}t+(r^2/4C_2t)]-(1/4)\pi i}\int_{-\infty}^{\infty}\frac{\left(\rho e^{-(3/4)\pi i}-\frac{r}{2C_2t}\right)e^{-C_2t\rho^2}}{(\omega_1+ix^{(3)}\beta-\omega_{c_2})+C_2\left(\rho e^{-(3/4)\pi i}-\frac{r}{2C_2t}\right)^2}d\rho.$$

(4) For the integration term in $A(t)$, we have

$$\mathbf{E}^{(4)}(\mathbf{r},t)=\frac{\mathbf{E}_{10}(\mathbf{r})}{\pi}\int_0^{\infty}\left[\frac{i^{1/2}\sqrt{x}E_{A1}^{(4)}(r,t)}{[M(x)\sqrt{\Omega_{c_1}}-i]^2-iM^2(x)x}+\frac{i^{-1/2}\sqrt{x}E_{B1}^{(4)}(r,t)}{[N(x)\sqrt{\Omega_{c_2}}+i]^2+iN^2(x)x}\right]dx$$
$$+\frac{\mathbf{E}_{20}(\mathbf{r})}{\pi}\int_0^{\infty}\left[\frac{i^{1/2}\sqrt{x}E_{A2}^{(4)}(r,t)}{[M(x)\sqrt{\Omega_{c_1}}-i]^2-iM^2(x)x}+\frac{i^{-1/2}\sqrt{x}E_{B2}^{(4)}(r,t)}{[N(x)\sqrt{\Omega_{c_2}}+i]^2+iN^2(x)x}\right]dx, \tag{D14}$$

with

$$E_{A1}^{(4)}(r,t)=e^{-i[\omega_{c_1}t-(r^2/4C_1t)]+(3/4)\pi i}\int_{-\infty}^{\infty}\frac{\left(\rho e^{(3/4)\pi i}+\frac{r}{2C_1t}\right)e^{-C_1t\rho^2}}{-x\beta+iC_1\left(\rho e^{(3/4)\pi i}+\frac{r}{2C_1t}\right)^2}d\rho,$$

$$E_{B1}^{(4)}(r,t)=\frac{\pi}{C_1}e^{(-i\omega_{c_2}-x\beta)t-r\sqrt{(\omega_{c_1}-\omega_{c_2}+ix\beta)/C_1}}\Theta\left(t-\frac{r}{2\sqrt{C_1}(\mathrm{Re}-\mathrm{Im})\sqrt{\omega_{c_1}-\omega_{c_2}+ix\beta}}\right)$$
$$+e^{-i[\omega_{c_1}t-(r^2/4C_1t)]+(3/4)\pi i}\int_{-\infty}^{\infty}\frac{\left(\rho e^{(3/4)\pi i}+\frac{r}{2C_1t}\right)e^{-C_1t\rho^2}}{i(\omega_{c_1}-\omega_{c_2})-x\beta+iC_1\left(\rho e^{(3/4)\pi i}+\frac{r}{2C_1t}\right)^2}d\rho,$$

$$E_{A2}^{(4)}(r,t)=-\frac{\pi}{C_2}e^{(-i\omega_{c_1}-x\beta)t-r\sqrt{(\omega_{c_1}-\omega_{c_2}-ix\beta)/C_2}}\Theta\left(t-\frac{r}{2\sqrt{C_2}(\mathrm{Re}+\mathrm{Im})\sqrt{\omega_{c_1}-\omega_{c_2}-ix\beta}}\right)$$
$$+e^{-i[\omega_{c_2}t+(r^2/4C_2t)]-(3/4)\pi i}\int_{-\infty}^{\infty}\frac{\left(\rho e^{-(3/4)\pi i}-\frac{r}{2C_2t}\right)e^{-C_2t\rho^2}}{-x\beta+i(\omega_{c_2}-\omega_{c_1})-iC_2\left(\rho e^{-(3/4)\pi i}-\frac{r}{2C_2t}\right)^2}d\rho,$$

$$E_{B2}^{(4)}(r,t)=e^{-i[\omega_{c_2}t+(r^2/4C_2t)]-(3/4)\pi i}\int_{-\infty}^{\infty}\frac{\left(\rho e^{-(3/4)\pi i}-\dfrac{r}{2C_2t}\right)e^{-C_2t\rho^2}}{-x\beta-iC_2\left(\rho e^{-(3/4)\pi i}-\dfrac{r}{2C_2t}\right)^2}d\rho.$$

APPENDIX E: THE CALCULATION OF THE EMISSION SPECTRUM S(r,ω)

The Fourier transform of the radiation field is

$$\mathbf{F}(\mathbf{r},\omega)=\frac{1}{2\pi}\int_0^{\infty}\mathbf{E}(\mathbf{r},t)e^{i\omega t}dt. \tag{E1}$$

So the emission spectrum $\mathbf{S}(\mathbf{r},\omega)$ can be obtained, $\mathbf{S}(\mathbf{r},\omega)=|\mathbf{F}(\mathbf{r},\omega)|^2$. From Eqs. (B11) and (D1), $\mathbf{F}(\mathbf{r},\omega)$ can be rewritten as the sum of four parts, which come from the four terms of Eq. (B11):

$$\mathbf{F}(\mathbf{r},\omega)=\mathbf{F}_1(\mathbf{r},\omega)+\mathbf{F}_2(\mathbf{r},\omega)+\mathbf{F}_3(\mathbf{r},\omega)+\mathbf{F}_4(\mathbf{r},\omega). \tag{E2}$$

(1) For the pure imaginary root $x^{(1)}$, we have

$$\begin{aligned}\mathbf{F}_1(\mathbf{r},\omega)=&\frac{\mathbf{E}_{10}(\mathbf{r})}{2\pi G'(x^{(1)})}\int_{-\infty}^{\infty}\frac{q_1e^{iq_1r}dq_1}{i(\omega_{q_1}-\omega_1)+x^{(1)}\beta}\int_0^{\infty}(e^{(x^{(1)}\beta-i\omega_1)t+i\omega t}-e^{-i\omega_{q_1}t+i\omega t})dt\\&+\frac{\mathbf{E}_{20}(\mathbf{r})}{2\pi G'(x^{(1)})}\int_{-\infty}^{\infty}\frac{q_2e^{iq_2r}dq_2}{i(\omega_{q_2}-\omega_1)+x^{(1)}\beta}\int_0^{\infty}(e^{(x^{(1)}\beta-i\omega_1)t+i\omega t}-e^{-i\omega_{q_2}t+i\omega t})dt\\=&\frac{\mathbf{E}_{10}(\mathbf{r})}{2\pi G'(x^{(1)})}\int_{-\infty}^{\infty}\frac{q_1e^{iq_1r}dq_1}{i(\omega_{q_1}-\omega_1)+x^{(1)}\beta}\lim_{s\to0^+}\left[\frac{-1}{-s+i(\omega-\omega_1-ix^{(1)}\beta)}-\frac{-1}{-s+i(\omega-\omega_{q_1})}\right]\\&+\frac{\mathbf{E}_{20}(\mathbf{r})}{2\pi G'(x^{(1)})}\int_{-\infty}^{\infty}\frac{q_2e^{iq_2r}dq_2}{i(\omega_{q_2}-\omega_1)+x^{(1)}\beta}\lim_{s\to0^+}\left[\frac{-1}{-s+i(\omega-\omega_1-ix^{(1)}\beta)}-\frac{-1}{-s+i(\omega-\omega_{q_2})}\right]\\=&\frac{\mathbf{E}_{10}(\mathbf{r})}{2\pi G'(x^{(1)})}\lim_{s\to0^+}\int_{-\infty}^{\infty}\frac{q_1e^{iq_1r}dq_1}{[-s+i(\omega-\omega_1-ix^{(1)}\beta)][-s+i(\omega-\omega_{q_1})]}\\&+\frac{\mathbf{E}_{20}(\mathbf{r})}{2\pi G'(x^{(1)})}\lim_{s\to0^+}\int_{-\infty}^{\infty}\frac{q_2e^{iq_2r}dq_2}{[-s+i(\omega-\omega_1-ix^{(1)}\beta)][-s+i(\omega-\omega_{q_2})]}\\=&-\frac{\mathbf{E}_{10}(\mathbf{r})}{2C_1G'(x^{(1)})}\lim_{s\to0^+}\frac{f_1(\omega)}{-s+i(\omega-\omega_1-ix^{(1)}\beta)}+\frac{\mathbf{E}_{20}(\mathbf{r})}{2C_2G'(x^{(1)})}\lim_{s\to0^+}\frac{f_2(\omega)}{-s+i(\omega-\omega_1-ix^{(1)}\beta)},\end{aligned} \tag{E3}$$

where $\Theta(x)$ is the step function. The functions $f_1(\omega)$ and $f_2(\omega)$ are defined as

$$f_1(\omega)=e^{-r\sqrt{(\omega_{c_1}-\omega)/C_1}}\Theta(\omega_{c_1}-\omega)+e^{ir\sqrt{(\omega-\omega_{c_1})/C_1}}\Theta(\omega-\omega_{c_1}),$$

$$f_2(\omega)=e^{-r\sqrt{(\omega-\omega_{c_2})/C_2}}\Theta(\omega-\omega_{c_2})+e^{-ir\sqrt{(\omega_{c_2}-\omega)/C_2}}\Theta(\omega_{c_2}-\omega).$$

(2) For the complex root $x^{(2)}=(a^{(2)}+ib^{(2)})/\beta$, we have $\omega_1-b^{(2)}<\omega_{c_2}$ and $a^{(2)}<0$.

$$\mathbf{F}_2(\mathbf{r},\omega)=-\frac{\mathbf{E}_{10}(\mathbf{r})}{2C_1K'(x^{(2)})}\frac{f_1(\omega)}{i(\omega-\omega_1-ix^{(2)}\beta)}+\frac{\mathbf{E}_{20}(\mathbf{r})}{2C_2K'(x^{(2)})}\frac{f_2(\omega)}{i(\omega-\omega_1-ix^{(2)}\beta)}. \tag{E4}$$

(3) For the complex root $x^{(3)}=(a^{(3)}+ib^{(3)})/\beta$, we have $\omega_1-b^{(3)}>\omega_{c_1}$ and $a^{(3)}<0$.

$$\mathbf{F}_3(\mathbf{r},\omega)=-\frac{\mathbf{E}_{10}(\mathbf{r})}{2C_1F'(x^{(3)})}\frac{f_1(\omega)}{i(\omega-\omega_1-ix^{(3)}\beta)}+\frac{\mathbf{E}_{20}(\mathbf{r})}{2C_2F'(x^{(3)})}\frac{f_2(\omega)}{i(\omega-\omega_1-ix^{(3)}\beta)}. \tag{E5}$$

(4) For the integration term in $A(t)$, we have

$$\mathbf{F}_4(\mathbf{r},\omega)=\frac{1}{\pi}\int_0^\infty\frac{-i^{1/2}\sqrt{x}dx}{[M(x)\sqrt{\Omega_{c_1}}-i]^2-iM^2(x)x}\left[\frac{\mathbf{E}_{10}(\mathbf{r})}{2C_1}\frac{f_1(\omega)}{i(\omega-\omega_{c_1}+ix\beta)}-\frac{\mathbf{E}_{20}(\mathbf{r})}{2C_2}\frac{f_2(\omega)}{i(\omega-\omega_{c_1}+ix\beta)}\right]$$
$$+\frac{1}{\pi}\int_0^\infty\frac{-i^{-1/2}\sqrt{x}dx}{[N(x)\sqrt{\Omega_{c_2}}+i]^2+iN^2(x)x}\left[\frac{\mathbf{E}_{10}(\mathbf{r})}{2C_1}\frac{f_1(\omega)}{i(\omega-\omega_{c_2}+ix\beta)}-\frac{\mathbf{E}_{20}(\mathbf{r})}{2C_2}\frac{f_2(\omega)}{i(\omega-\omega_{c_2}+ix\beta)}\right]. \tag{E6}$$

APPENDIX F: PROOF OF $V_e^{(2)}>V_{f2}^{(2)}$ AND $V_e^{(3)}>V_{f1}^{(3)}$

1. Proof of $v_e^{(2)}>v_{f2}^{(2)}$

When the upper level is within region II, we have the complex root $x^{(2)}=(a^{(2)}+ib^{(2)})/\beta$ with $\omega_1-b^{(2)}<\omega_{c_2}$, and $a^{(2)}<0$.

Suppose

$$\sqrt{\omega_1-\omega_{c_2}+ix^{(2)}\beta}=p-iq. \tag{F1}$$

So we can obtain

$$p^2-q^2=\omega_1-\omega_{c_2}-b^{(2)},$$
$$pq=-a^{(2)}/2, \tag{F2}$$

and $q>p>0$ due to $\omega_1-\omega_{c_2}-b^{(2)}<0$ and $a^{(2)}<0$. The energy velocity $v_e^{(2)}$ and the front velocity $v_{f2}^{(2)}$ can be written as

$$v_e^{(2)}=-a^{(2)}\sqrt{C_2}/\mathrm{Re}(\sqrt{\omega_1-\omega_{c_2}+ix^{(2)}\beta})=-a^{(2)}\sqrt{C_2}/p, \tag{F3}$$

and

$$v_{f2}^{(2)}=-2\sqrt{C_2}(\mathrm{Im}+\mathrm{Re})\sqrt{\omega_1-\omega_{c_2}+ix^{(2)}\beta}$$
$$=-2\sqrt{C_2}(p-q). \tag{F4}$$

So we have

$$v_{f2}^{(2)}=-2\sqrt{C_2}(p-q)$$
$$=-2\sqrt{C_2}p-\sqrt{C_2}a^{(2)})/p$$
$$=-2\sqrt{C_2}p+v_e^{(2)}<v_e^{(2)}. \tag{F5}$$

2. Proof of $v_e^{(3)}>v_{f1}^{(3)}$

Similarly, there is the complex root $x^{(3)}=(a^{(3)}+ib^{(3)})/\beta$ with $\omega_1-b^{(3)}>\omega_{c_1}$, and $a^{(3)}<0$ as the upper level is within region III. Suppose

$$\sqrt{\omega_{c_1}-\omega_1-ix^{(3)}\beta}=p+iq. \tag{F6}$$

We have

$$p^2-q^2=\omega_{c_1}-\omega_1+b^{(3)},$$
$$pq=-a^{(3)}/2, \tag{F7}$$

and $q>p>0$ due to $\omega_{c_1}-\omega_1+b^{(3)}<0$ and $a^{(3)}<0$. The energy velocity $v_e^{(3)}$ and the front velocity $v_{f1}^{(3)}$ can be rewritten as follows:

$$v_e^{(3)}=-a^{(3)}\sqrt{C_1}/\mathrm{Re}(\sqrt{\omega_{c_1}-\omega_1-ix^{(3)}\beta})$$
$$=-a^{(3)}\sqrt{C_1}/p, \tag{F8}$$

$$v_{f1}^{(3)}=2\sqrt{C_1}(\mathrm{Im}-\mathrm{Re})\sqrt{\omega_{c_1}-\omega_1-ix^{(3)}\beta}$$
$$=2\sqrt{C_1}(q-p). \tag{F9}$$

In results, we obtain

$$v_{f1}^{(3)}=2\sqrt{C_1}(q-p)$$
$$=a^{(3)}\sqrt{C_1}/p-2\sqrt{C_1}p$$
$$=v_e^{(3)}-2\sqrt{C_1}p<v_e^{(3)}. \tag{F10}$$

[1] E. Yablonovitch, Phys. Rev. Lett. **58**, 2059 (1987); E. Yablonovitch, T.J. Gmitter, and K.L. Leung, *ibid.* **67**, 2295 (1991).

[2] S. John, Phys. Rev. Lett. **58**, 2486 (1987).

[3] E. Yablonovitch, J. Opt. Soc. Am. B **10**, 283 (1993); J. D. Joannopoulos, R. D. Meade, and J. N. Winn, *Photonic Crystals* (Princeton, New York, 1995).

[4] S. John and T. Quang, Phys. Rev. A **50**, 1764 (1994).

[5] S. John and J. Wang, Phys. Rev. Lett. **64**, 2418 (1990); Phys. Rev. B **43**, 12 772 (1991); S. John and T. Quang, Phys. Rev. Lett. **74**, 3419 (1995); **76**, 1320 (1996); **78**, 1888 (1997); N.

Vats, S. John, and K. Busch, Phys. Rev. A **65**, 043808 (2002).
[6] S. Bay, P. Lambropoulos, and K. Molmer, Phys. Rev. Lett. **79**, 2654 (1997); Opt. Commun. **132**, 237 (1996); **146**, 130 (1998); P. Lambropoulos *et al.*, Rep. Prog. Phys. **63**, 455 (2000); G.M. Nikolopoulos and P. Lambropoulos, Phys. Rev. A **61**, 053812 (2000).
[7] S.-Y. Zhu, H. Chen, and H. Huang, Phys. Rev. Lett. **79**, 205 (1997); S.-Y. Zhu *et al.*, *ibid.* **84**, 2136 (2000); Y.P. Yang *et al.*, Opt. Commun. **182**, 349 (2000); Y.P. Yang and S.-Y. Zhu, Phys. Rev. A **62**, 013805 (2000); J. Mod. Opt. **47**, 1513 (2000); S.-Y. Zhu *et al.*, Europhys. Lett. **62**, 210 (2003).
[8] A.G. Kofman, G. Kurizki, and B. Sherman, J. Mod. Opt. **41**, 353 (1994); S. Bay, P. Lambropoulos, and K. Molmer, Phys. Rev. A **55**, 1485 (1997).
[9] Y.P. Yang and S.-Y. Zhu, Phys. Rev. A **61**, 043809 (2000); Y.P. Yang *et al.*, Opt. Commun. **193**, 153 (2001); S.-Y. Xie, Y.P. Yang, and X. Wu, Eur. Phys. J. D **13**, 129 (2001).
[10] T. Quang *et al.*, Phys. Rev. Lett. **79**, 5238 (1997).
[11] Y.P. Yang *et al.*, Phys. Lett. A **270**, 41 (2000); D.G. Angelakis, E. Paspalakis, and P.L. Knight, Phys. Rev. A **64**, 013801 (2001); H.Z. Zhang *et al.*, *ibid.* **65**, 063802 (2002).
[12] A.G. Kofman and G. Kurizki, Phys. Rev. A **54**, R3750 (1996); M. Lewenstein and K. Rzazewski, *ibid.* **61**, 022105 (2000).
[13] E.P. Petrov *et al.*, Phys. Rev. Lett. **81**, 77 (1998); M. Megens *et al.*, Phys. Rev. A **59**, 4727 (1999); J. Opt. Soc. Am. B **16**, 1403 (1999); H.P. Schriemer *et al.*, Phys. Rev. A **63**, 011801(R) (2001).
[14] M. O. Scully and M. S. Zubairy, *Quantum Optics* (Cambridge University Press, Cambridge, 1997), Chap. 6.
[15] J. Callaway, *Quantum Theory of the Solid State* (Academic Press, New York, 1976), Chap. 5.